Integrated stratigraphic studies of Paleocene–lowermost Eocene sequences, New Jersey Coastal Plain: Evidence for glacioeustatic control

Ashley D. Harris,[1,2] Kenneth G. Miller,[1] James V. Browning,[1] Peter J. Sugarman,[3] Richard K. Olsson,[1] Benjamin S. Cramer,[4] and James D. Wright[1]

Received 21 May 2009; revised 7 March 2010; accepted 2 April 2010; published 31 August 2010.

[1] We describe seven Paleocene to lowermost Eocene sequences in core holes at Island Beach, Bass River, Ancora, Millville, and Sea Girt, NJ (Ocean Drilling Program Leg 150X, 174AX) and analyze benthic foraminiferal assemblages to assess paleodepth changes within sequences. These sequences are referred to as Pa0, Pa1a, Pa1b, Pa2a, Pa2b, Pa3a, and Pa3b. Paleocene sequence boundaries are identified by unconformities and variations in benthic foraminiferal biofacies. We used Q-mode factor analysis and paleoslope modeling to identify three distinct middle-outer neritic benthic foraminiferal assemblages and their associated water depths. Paleodepths during the early Paleocene and deposition of Pa0, Pa1a, and Pa2b were ~80 m with ~20 m changes across sequence boundaries. A long-term shallowing occurred through the late Paleocene where paleodepths were ~50–70 m in Pa3a. This trend drastically changes in the earliest Eocene where the paleodepths of sequence Pa3b were ~120–150 m. New Jersey Paleocene sequence boundaries correlate with those in other regions and with $\delta^{18}O$ increases in the deep sea, suggesting Paleocene eustatic lowerings were associated with ice-growth events.

Citation: Harris, A. D., K. G. Miller, J. V. Browning, P. J. Sugarman, R. K. Olsson, B. S. Cramer, and J. D. Wright (2010), Integrated stratigraphic studies of Paleocene–lowermost Eocene sequences, New Jersey Coastal Plain: Evidence for glacioeustatic control, *Paleoceanography*, *25*, PA3211, doi:10.1029/2009PA001800.

1. Introduction

[2] The Paleocene to early Eocene (65–50 Ma) was one of the warmest intervals of the past 100 Myr, exceeded only by the Late Cretaceous [*Zachos et al.*, 2001; *Miller et al.*, 2005a, 2005b]. Intervals of the Late Cretaceous to Eocene is considered to have been a "Greenhouse World" with high CO_2 [e.g., *Royer et al.*, 2004], warm deep water [e.g., *Miller et al.*, 1987, 2005b], and warm high latitudes [e.g., *Savin et al.*, 1975; *Savin*, 1977; *Shackleton and Boersma*, 1981; *Miller et al.*, 2005a, 2005b]. However, *Haq et al.* [1987] reported several rapid Paleocene sea level changes of 150 m, each in less than 1 Myr. This poses a dilemma because large scale, rapid sea level changes are only attributable to ice-volume changes [e.g., *Pitman and Golovchenko*, 1983] and this interval has been presumed to be ice-free. To help explain this apparent contradiction, *Miller et al.* [2003, 2004, 2005a] attributed Myr scale sea level changes in the Greenhouse World to growth and decay of ephemeral small- to medium-sized ice sheets (8–12 × 10^6 km^3 (20–30 m glacioeustatic equivalent) [see *DeConto and Pollard*, 2003]).

[3] New Jersey is an ideal passive continental margin to study Cenozoic sea level changes because of its simple subsidence history [*Steckler and Watts*, 1978; *Kominz et al.*, 1998] and excellent chronostratigraphic control [e.g., *Olsson and Wise*, 1987a, 1987b] (Figure 1). Sediment supply was low to moderate in the Paleocene [*Poag and Sevon*, 1989; *Miller et al.*, 2004] which minimizes the effect of sediment supply changing the strandline position or accommodation.

[4] Previous studies by *Olsson and Wise* [1987a, 1987b] and *Olsson* [1991] delineated Paleocene sea level changes in the New Jersey Coastal Plain to test the eustatic amplitude estimates of *Haq et al.* [1987]. However, their study was limited to discontinuous drill sections and outcrops and did not account for the effects of sediment loading and basin subsidence. Their studies of Deep Sea Drilling Project (DSDP) sites on the New Jersey deepwater continental slope (Sites 605 and 612) were conducted on continuously cored material, but were restricted to deep water sites where direct evidence of sea level change is lacking [*Olsson and Wise*, 1987a]. They identified two sequences in the lower Paleocene Hornerstown Formation and a mid-Paleocene sequence that straddles the Hornerstown and Vincentown formational boundary. *Olsson and Wise* [1987a, 1987b] also identified a thin uppermost Paleocene sequence consisting of clay, silt, and sand. Lithologic and biofacies analysis indicated that the upper Paleocene unconformities correlated well with

[1]Department of Earth and Planetary Sciences, Rutgers, State University of New Jersey, Piscataway, New Jersey, USA.
[2]Now at Chevron Corporation, Houston, Texas, USA.
[3]New Jersey Geological Survey, Trenton, New Jersey, USA.
[4]Department of Geological Sciences, University of Oregon, Eugene, Oregon, USA.

0883-8305/10/2009PA001800

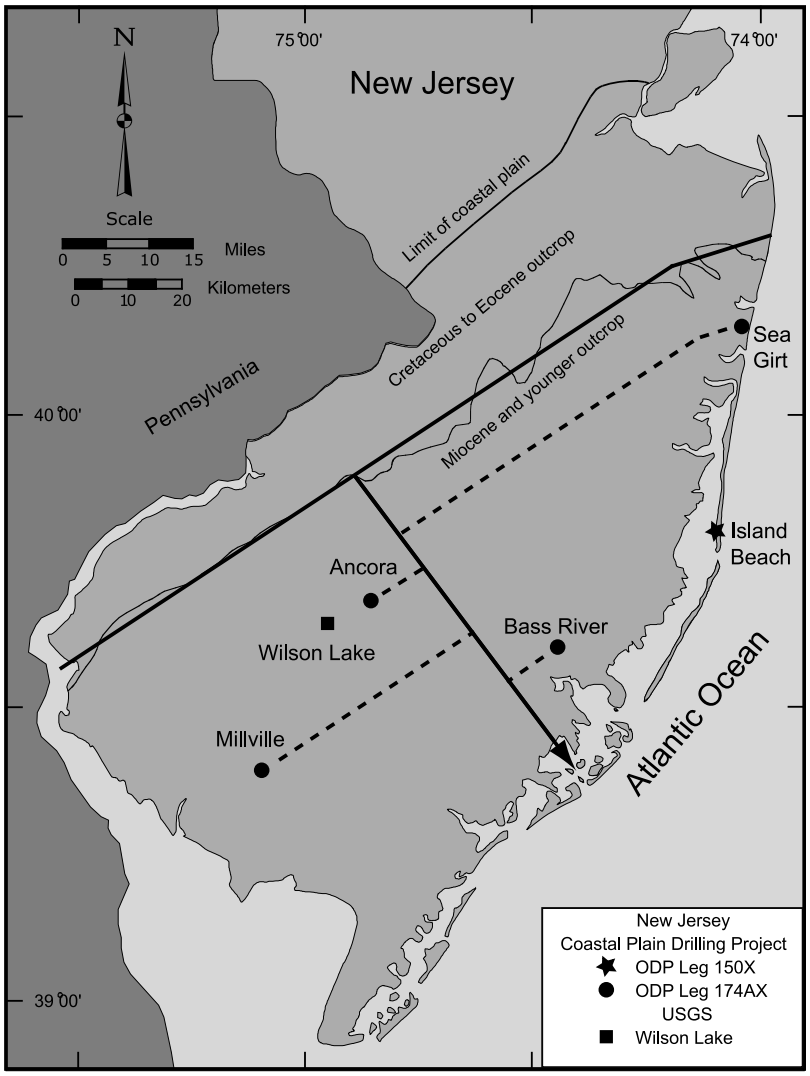

Figure 1. Location map of boreholes studied. The arrow perpendicular to Cenozoic outcrop denotes the dip direction of Paleocene strata. Dashed lines show the locations of core holes projected onto the dip-line used in paleoslope modeling.

cycles TA2.1 and 2.3 of *Haq et al.* [1987]. Biofacies characterization and paleoslope modeling by *Olsson and Wise* [1987b] showed water depth changes of ~55 m during the Paleocene, which was significantly less than the 150 m eustatic changes estimated by *Haq et al.* [1987].

[5] *Liu et al.* [1997] used continuously sampled core from Island Beach, New Jersey (ODP Leg 150X) to identify three Paleocene sequences (Pa1, Pa2, and Pa3) and characterize associated paleodepth changes (Pa0, Pa2a, and Pa3a of this study). The sequences of *Liu et al.* [1997] are correlative with *Olsson and Wise*'s [1987a, 1987b] placement of sequences in the Hornerstown Formation and Vincentown Formations. *Liu et al.* [1997] determined that the Paleocene unconformities at Island Beach correlated well with the TA1.1/1.2 and TA2.2/2.3/2.4 cycles of *Haq et al.* [1987]. Biofacies analysis of benthic foraminifera also detailed relatively small amplitude water-depth changes during the Paleocene.

[6] There is considerable interest by the general public and scientific community in sea level changes associated with greenhouse warming, particularly the Paleocene Eocene Thermal Maximum (PETM) and Eocene Thermal Maximum 2 (ETM2) [*Sluijs et al.*, 2008]. The terrestrial, oceanic, and atmospheric changes associated with the PETM are seen as possible analogs to today's global conditions. The PETM was a brief event (~30–200 kyr) [*Bains et al.*, 1999; *Röhl et al.*, 2000; *Farley and Eltgroth*, 2003] of extreme global warmth (4–6°C) superimposed on a warm climatic interval of the late Paleocene–early Eocene (ca. 56–50 Ma). The PETM is identified in marine and terrestrial records by a negative carbon isotope excursion (CIE) of ~3–4‰ [e.g., *Kennett and Stott*, 1991; *Cramer et al.*, 1999; *Zachos et al.*, 2001], a deep-ocean benthic foraminiferal extinction [e.g., *Thomas*, 1990; *Katz and Miller*, 1991; *Pak and Miller*, 1992], and a mammalian turnover [*Gingerich*, 2003]. The principal cause of this global event is still debated. Primary

mechanisms or accompanying positive feedbacks include: massive methane release [e.g., *Dickens et al.*, 1995; *Katz et al.*, 2001; *Thomas et al.*, 2002], widespread burning of peat [e.g., *Kurtz et al.*, 2003], bolide impact [e.g., *Kent et al.*, 2003], and volcanic activity [e.g., *Eldholm and Thomas*, 1993; *Svensen et al.*, 2004; *Storey et al.*, 2007].

[7] *Sluijs et al.* [2008] delineated relative sea level changes associated with the PETM in the North Sea, New Zealand and New Jersey (Bass River and Wilson Lake, NJ). They assembled a high-resolution record of dinocysts, terrestrially derived organic matter, and grain size to infer relative sea level changes and identified two sequence boundaries bracketing the PETM. They inferred an inner neritic environment with relative shallowing toward the CIE followed by a sharp increase in water depth just below and at the CIE. Paleoecologic and grain size analyses indicate relatively deeper outer neritic environments at the CIE and throughout the lowermost Eocene. *Sluijs et al.* [2008] attributed the eustatic high of the PETM to melting of a small Antarctic ice sheet, thermal expansion of the ocean, and tectonic influence from the North Atlantic Igneous Province.

[8] In this paper, we present a detailed paleodepth and sequence stratigraphic history for the Paleocene–lowermost Eocene of the New Jersey Coastal Plain of integrating biostratigraphic, paleoecologic, and sequence stratigraphic studies. Utilizing continuously drilled core holes from Bass River, Ancora, Millville, and Sea Girt, NJ (ODP Leg 174 AX; Figure 1) we: 1) identified benthic foraminiferal biofacies using factor analysis; 2) inferred water depth changes based on benthic foraminiferal biofacies, percent planktonic foraminifera, lithofacies and paleoslope modeling; and 3) recognized 7 Paleocene–lowermost Eocene sequences. We were able to derive a more complete record of sea level change for the interval from ~65–55 Ma. We also compare the timing of the development of sequence boundaries in NJ to those in other well known Paleocene sections and to the deep sea oxygen isotope record to invoke a glacioeustatic mechanism for sequence development.

2. Methods

2.1. Interpretive Framework for Sequences

[9] Paleocene–earliest Eocene successions on the New Jersey Coastal Plain comprise the Hornerstown Formation and Vincentown Formation, and a gray kaolinitic clay unit. The Hornerstown Formation is a heavily burrowed, fine to medium, glauconitic sand to glauconitic clay. The Vincentown Formation is a fine to coarse, quartzose, sometimes silty, glauconitic sand. The history of the lithostratigraphy and placement of the unnamed clay is complicated [*Gibson et al.*, 1993; *Olsson and Wise*, 1987a, 1987b]. Previous workers have included the gray kaolinitic clay unit as a part of the Vincentown Formation or the lower Eocene Manasquan Formation. However, *Olsson and Wise* [1987a, 1987b] and *Cramer et al.* [1999] noted the massive gray kaolinitic clay unit is markedly different from the glauconitic green clay of the Manasquan Formation above and the glauconite sand of the Vincentown Formation below. The unnamed clay unit is lithologically similar to the Marlboro Clay outcropping in Maryland and Virginia, suggesting a much larger regional extent of the clay. Additionally, the Marlboro Clay is stratigraphically significant because it was deposited during the Paleocene-Eocene Thermal Maximum [*Gibson et al.*, 1993; *Kopp et al.*, 2009]. We apply the term Marlboro Clay to refer to the gray clay unit in the New Jersey sections. The Marlboro Clay is identified by a ~4‰ decrease in $\delta^{13}C$ that marked the CIE and Paleocene Eocene Thermal Maximum (PETM) near the base [e.g., *Cramer et al.*, 1999; *Zachos et al.*, 2006; *John et al.*, 2008], thus identifying it as a lower Eocene formation [*Aubry et al.*, 2000, 2007].

[10] Unconformities were identified based on biostratigraphic breaks, erosional surfaces, rip–up clasts, burrowed surfaces, and other variations in lithology (Figure 2). New Jersey Paleocene–lowermost Eocene sequences display a stacked pattern of the shallow water facies of the highstand system tract (HST) overlying deeper water facies of the transgressive systems tract (TST). Lowstand system tracts (LST) are absent in Paleocene–lowermost Eocene sequences and in most of the 100 Myr record of the New Jersey coastal plain [*Browning et al.*, 2008]. Typical New Jersey Paleocene–lowermost Eocene sequences are comprised of basal glauconitic clays representing the transgressive surface (TST), coarsening up to quartzose, glauconitic silts and sands (HST). The sequences were further evaluated using benthic foraminiferal biofacies derived from population abundances, factor analysis, and other statistics of foraminifera. The mid-Paleocene sections at Ancora and Millville yielded rare and poorly preserved nannofossils and planktonic foraminifers and thick barren zones due to dissolution. Many of the Paleocene samples at Sea Girt contained too few benthic foraminifers to allow statistical analysis. We attribute poor preservation to its up dip location. Paleodepths from Sea Girt are largely derived from lithology and the bathymetric zonation of the benthic foraminifers identified. Thus, for the purposes of this paper we focused on more complete sections at Bass River, Ancora, and Millville, NJ. We also compare these studies with the published New Jersey records at Island Beach [e.g., *Liu et al.*, 1997].

2.2. Faunal Analysis

[11] Samples of 18–40 g were taken at 1–5 ft (30–150 cm) intervals at each core hole. The samples were disaggregated by soaking in a sodium metaphosphate solution to disaggregate them and washed through a 63 μm sieve to remove the clay-silt fraction and dried.

[12] Samples were dry sieved through a 105 μm screen so comparisons could be made with earlier studies [*Liu et al.*, 1997]. Samples with large numbers of foraminifers were split in a micro-splitter to obtain approximately 300 total foraminifers.

[13] Benthic foraminifers are sensitive to a number of environmental factors that vary with depth including oxygen, food sources, salinity, temperature, light, and current strength [*Bandy and Arnal*, 1960; *Poag*, 1980; *Van der Zwaan et al.*, 1999]. Thus, benthic foraminiferal assemblages are useful indicators of sequence boundaries, which are associated with change in paleobathymetry [*Browning et al.*, 1997; *Olsson and Wise*, 1987a].

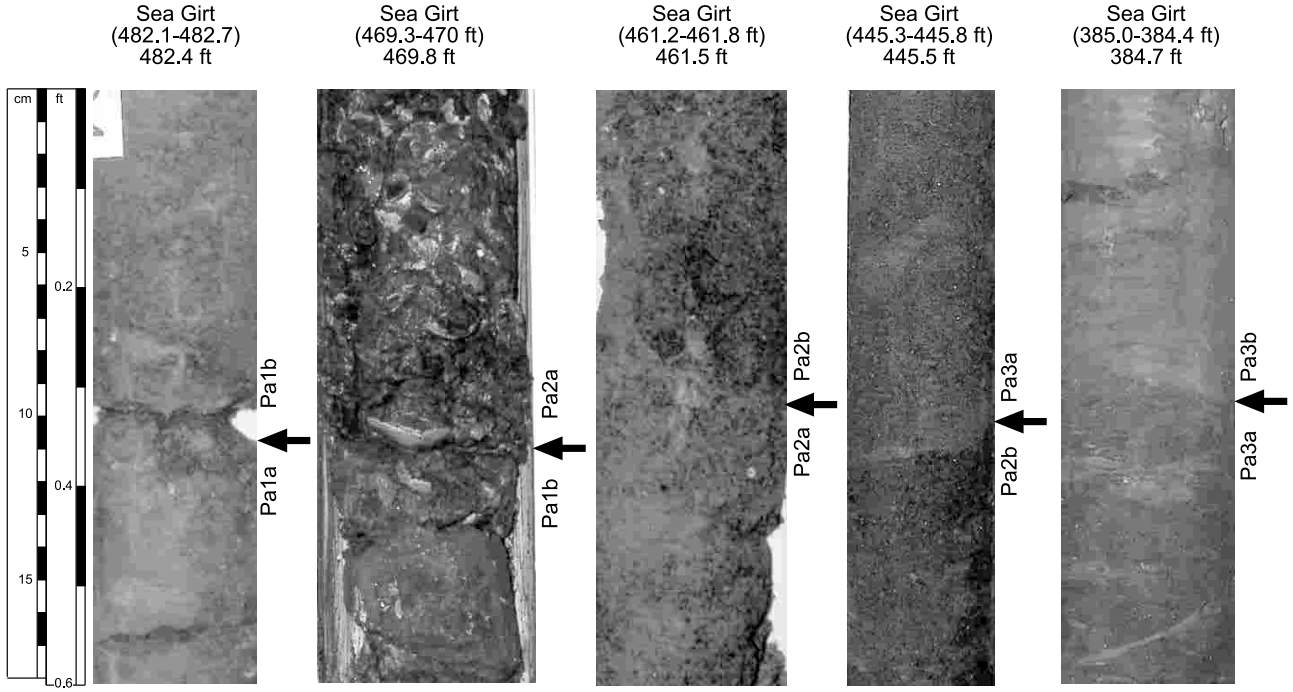

Figure 2. Photographs of sequence boundaries from the Sea Girt core. Arrows represent sequence boundary location.

[14] Q-mode factor analysis was used to identify natural assemblages of benthic foraminifers and compare variations among the samples at Ancora, Bass River, Millville and Sea Girt. A normalized data set of 56 samples with a minimum of 50 specimens each were imported into Systat 5.2.1 to perform principal component analysis with varimax rotation. Three principal components were extracted and rotated. Factor loadings above 0.5 were considered significant. The tolerance value was set at 0.001, iterations at 25, and eigenvalue at 0. Three principal components with eigenvalues (latent roots) >1 were extracted and rotated. The rotated principal components accounted for 51% of the faunal variation. All three factors have stratigraphic significance in the core holes.

3. Results

3.1. Benthic Foraminiferal Biofacies

[15] The three biofacies of benthic foraminifers identified by factor analysis are representative of middle to outer neritic environments (50–150 m; Figure 3). For this study we used the bathymetric zonation of *van Morkhoven et al.* [1986]: 0–30 m, inner neritic; 30–100 m, middle neritic; 100–200 m, outer neritic; 200–2000 m, bathyal. Benthic foraminifers were identified to the species level using the taxonomy of *Berggren and Aubert* [1975], *Brotzen* [1948], *Plummer* [1926], *Cushman* [1951], and *van Morkhoven et al.* [1986].

3.1.1. Biofacies A

[16] Factor 1 (biofacies A) is dominated by *Stensioeina* cf. *beccariiformis parvula* (6.53 score), *Bulimina midwayensis* (1.63 score), *Osangularia plummerae* (1.45 score), *Gaudryina pyramidata* (1.32 score), and *Cibicidoides succedens* (1.30 score; Table 1).

[17] *Stensioeina* cf. *beccariiformis parvula* is a middle to outer shelf morphotype of the deeper water *Stensioeina beccariiformis* [*van Morkhoven et al.*, 1986]. This suggests the paleodepth for Biofacies A is middle-outer neritic paleoenvironments. Additionally, biofacies A is dominant in sediments with relatively low percent planktonic foraminifera (10–40%) and relatively higher amounts of quartz sand at Bass River and Ancora; generally more common in the highstand systems tracts.

3.1.2. Biofacies B

[18] Factor 2 (biofacies B) is comprised of *Pulsiphonina prima* (5.94 score), *Anomalinoides acuta* (3.83 score), *Spiroplectammina plummerae* (1.8 score), *Angulogerina cuneata* (1.05 score), and *Bulimina hornerstownensis* (1.04 score). Biofacies B is indicative of slightly deeper water than biofacies A, because it is dominant in intervals with higher percentages of planktonic foraminifera (75–90%) and more mud-rich lithology. We assign biofacies B to outer neritic paleoenvironments.

3.1.3. Biofacies C

[19] Factor 3 (biofacies C) is dominated by *Tappanina selmensis* (7.72 score), *Ellipsonodosaria paleocenica* (2.18), *Trifarina herberti* (1.2 score) and *Nodosaria* cf. *N. longiscata* (1.17 score). *T. selmensis* would normally indicate that biofacies C is outer shelf [*Berggren and Aubert*, 1975; *Olsson and Wise*, 1987b]. However, this biofacies C does not correlate with the highest peaks in percent planktonic foraminifera. *Tappanina selmensis* is the only significant taxon that dominates in biofacies C (Table 1). We assign biofacies C to middle neritic paleoenvironments because it

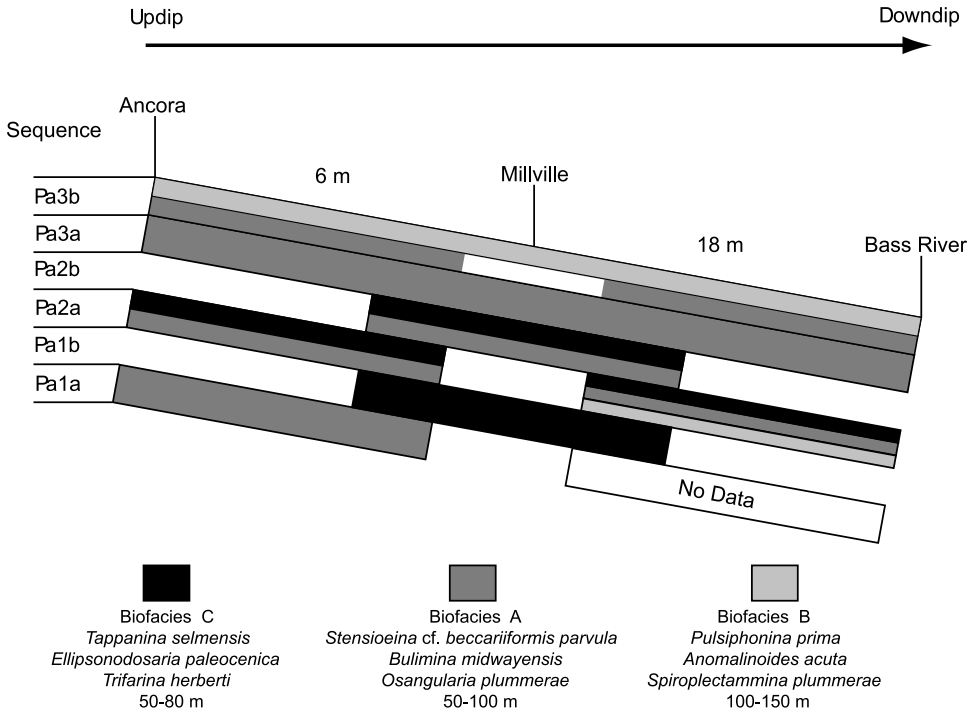

Figure 3. The spatial distribution of benthic foraminiferal biofacies within each sequence on paleoslope (1:1000). Blank areas denote where sequences were not identified at respective boreholes. Values between sites indicate the vertical distance between sites. The vertical and horizontal distance between each borehole projected on the paleoslope line is not to scale.

is associated with low percent planktonic foraminifera and typically overlies biofacies A (Figure 3).

3.2. Paleobathymetry Estimates

[20] Paleoslope modeling is based on the concept that benthic foraminiferal biofacies occupy distinct environments horizontally, but overlap and replace each other vertically as depositional environments change [*Johnson*, 1972], following Walther's Law of Facies. This implies that deeper water biofacies are located in the lower part of the sequence (TST) and are overlain by shallower biofacies (HST) [*Olsson and Nyong*, 1984; *Browning et al.*, 1997] (Figures 3 and 4). Examining the spatial relationships of the biofacies allows us to determine relative water depth changes between each biofacies and within each sequence (Figure 3). The best example is displayed in sequence Pa2a at Bass River, NJ. Biofacies B dominates the base of the sequence and followed by biofacies A and biofacies C at the top. Sequences Pa2a and Pa2b at Ancora and Millville, respectively, display similar patterns with biofacies A overlain by biofacies C.

[21] Paleodepth values are assigned by integrating the biostratigraphic and sequence stratigraphic data and projecting them onto a paleodip profile [*Olsson and Nyong*, 1984].

[22] The dip profile was derived from locating the strike of Paleocene outcrops and using a 1:1000 gradient (Figure 1). This profile is the physiographic gradient of the New Jersey Coastal Plain derived from 2 dimensional backstripping during the Paleocene [e.g., *Steckler et al.*, 1999] and is similar to the modern gradient. Paleoslope modeling provides a measurement of the vertical difference between sites. According to this model paleodepths at Ancora, Millville and Bass River are 6 m, 12 m and 30 m deeper, respectively, than the most updip site (Sea Girt; Figure 3).

[23] The lack of nearshore sediments in outcrop or updip core hole sites adds a level of uncertainty in assigning absolute paleodepths to these sequences. However, we assume a minimum depth estimate at our updip sites of ~50 m based on the benthic foraminiferal biofacies, and fine to medium quartz glauconitic lithology [*Olsson and Wise*, 1987b]. Generally, Paleocene sequences consist of basal glauconite clays overlain by silty quartzose glauconite sand. Additionally, percent planktonic foraminifera decrease toward the top of the sequence. This suggest paleodepths changes within each sequence is ~20 m. Based on depth zonation, paleodepth modeling, and sequence stratigraphic analysis, we assign paleodepths of 50–80 m for the middle neritic biofacies C. Biofacies A occupied similar paleodepths, but is assigned to slightly deeper middle neritic environments (50–100 m) based on higher percent planktonic foraminifera and its spatial relationship with biofacies C (Figure 3). Biofacies B, is an outer neritic biofacies associated with high percent planktonic foraminifera and clay-rich lithology is assigned to 100–150 m water depths. This integrated stratigraphic approach provides a paleobathymetric distribution of each sequence with corresponding benthic foraminiferal biofacies (Figure 4). This data set is an

Table 1. Factor Scores of the Top 50 Most Dominant Benthic Foraminifer Species for Biofacies A, B, and C at Bass River, Ancora, and Millville[a]

Species	Factor Score
Biofacies A	
Stensioeina cf. *beccariiformis parvula*	6.53
Bulimina midwayensis	1.63
Osangularia plummerae	1.45
Gaudryina pyramidata	1.32
Cibicidoides succedens	1.30
Anomalinoides welleri	1.16
Cibicidoides alleni	0.94
Stilostomella plummerae	0.79
Spiroplectammina mexiaensis	0.26
Pullenia quinqueloba	0.16
Angulogerina cuneata	0.14
Ellipsonodosaria plummerae	0.09
Nodosarella attenuata	0.05
Dentalina? pseudoaculeata	0.00
Eponides plummerae	−0.01
Stilostomella sp. A	−0.02
Dentalina nasuta	−0.02
Dentalina sp. A	−0.05
Nodosarella paleocenica	−0.05
Cornuspira sp. A	−0.06
Nodosaria macneili	−0.06
Saracenaria trigonata	−0.06
Allomorphina paleocenica	−0.07
Dentalina alabamensis	−0.07
Stilostomella paleocenica	−0.07
Lagena laevis	−0.08
Lenticulina turbinata	−0.08
Marginulinopsis tuberculata	−0.08
Marginulina sp. A	−0.09
Dentalina eocenica	−0.09
Dentalina insulsa	−0.09
Nodosaria sp. B	−0.09
Dentalina sp. B	−0.09
Ramulina spp.	−0.09
Dentalina pseudo-obliquestriata	−0.09
Vaginulina? sp. A	−0.09
Dentalina plummerae	−0.09
Loxostomoides applinae	−0.10
Quadrimorphina allomorphinoides	−0.10
Guttulina sp. A	−0.10
Polymorphinella cf. *P. elongata*	−0.10
Globulina gibba	−0.10
Nodosaria affinis	−0.10
Biofacies B	
Pulsiphonina prima	5.94
Anomalinoides acuta	3.83
Spiroplectammina plummerae	1.80
Angulogerina cuneata	1.05
Bulimina hornerstownensis	1.04
Angulogerina wilcoxensis	0.67
Gyroidinoides octocamerata	0.52
Lenticulina orbicularis	0.41
Bulimina aspero-aculeata	0.15
Alabamina wilcoxensis	0.09
Gyroidinoides subangulata	0.09
Bolivina midwayensis	0.08
Cibicides howelli	0.03
Bulimina paleocenica	0.01
Turrilina brevispira	−0.02
Bulimina ovata	−0.05
Globulina gibba	−0.06
Bulimina cacumenata	−0.07
Loxostomum sp. A	−0.07
Eponides elevatus	−0.07
Bulimina kugleri	−0.08
Nodosaria longiscata	−0.08
Lagena sulcata	−0.08
Uvigerina sp. A	−0.08
Dentalina wilcoxensis	−0.09
Anomalinoides midwayensis	−0.10
Cibicidoides incognita	−0.10
Nonionella sp. A	−0.10
Bulimina sp. A	−0.10
Dentalina colei	−0.10
Pleurostomella alternans	−0.10
Polymorphinella cf. *P. elongata*	−0.10
Spiroplectammina rossae	−0.10
Chrysalogonium arkansanum	−0.10
Nonion sp. A	−0.10
Dentalina plummerae	−0.10
Nodosaria granti	−0.10
Pseudoglandulina sp. A	−0.10
Lenticulina semicostata	−0.10
Planularia toddae	−0.10
Stilostomella paleocenica	−0.10
Loxostomoides applinae	−0.10
Stilostomella midwayensis	−0.10
Biofacies C	
Tappanina selmensis	7.72
Ellipsonodosaria paleocenica	2.18
Trifarina herberti	1.20
Nodosaria cf. *N. longiscata*	1.17
Bulimina aspero-aculeata	1.09
Bulimina hornerstownensis	0.52
Cibicidoides succedens	0.37
Gavelinella danica	0.36
Lenticulina rotulata	0.24
Cibicides howelli	0.22
Gyroidinoides subangulata	0.18
Turrilina brevispira	0.13
Bulimina sp. B	0.05
Anomalinoides midwayensis	0.04
Gavelinella lellingensis	0.03
Cibicidoides sp. A	0.00
Spiroplectammina mexiaensis	−0.02
Ellipsonodosaria midwayensis	−0.03
Dentalina? pseudoaculeata	−0.04
Quadrimorphina allomorphinoides	−0.05
Ramulina spp.	−0.06
Dentalina aculeata	−0.07
Eponides plummerae	−0.07
Cibicidoides incognita	−0.07
Nonion sp. A	−0.07
Allomorphina paleocenica	−0.07
Nodosaria longiscata	−0.08
Pullenia quinqueloba	−0.08
Uvigerina sp. A	−0.08
Bulimina sp. A	−0.08
Pleurostomella paleocenica	−0.08
Spiroplectammina rossae	−0.08
Marginulina sp. B	−0.08
Planularia toddae	−0.09
Lagena sulcata	−0.09
Nonionella sp. A	−0.09
Bulimina quadrata	−0.09
Entosolenia sp. A	−0.09
Glandulina sp. A	−0.09
Nonionella soldadoensis	−0.09
Guttulina sp. A	−0.09
Nodosaria plummerae	−0.09
Palmula robusta	−0.09

[a]Dominant species have high factor values.

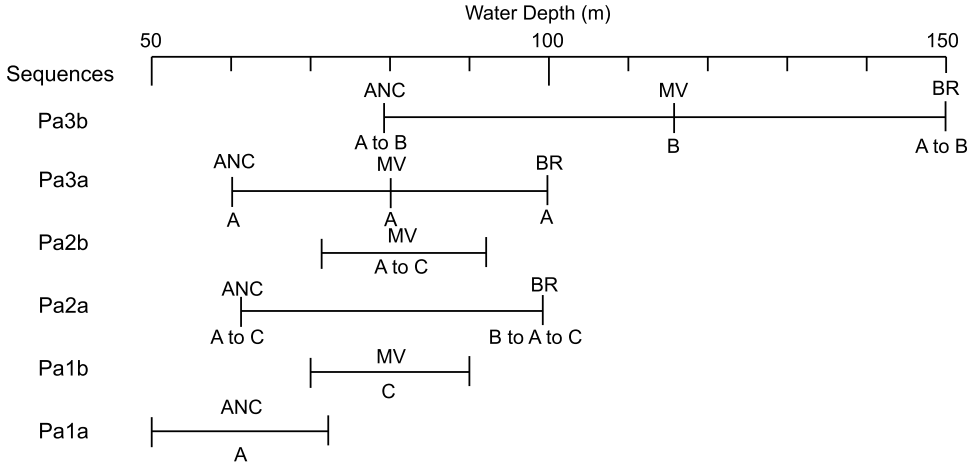

Figure 4. Paleobathymetric distribution of each sequence with benthic foraminiferal biofacies stacking pattern at each site based on paleoslope modeling. ANC, Ancora; BR, Bass River; and MV, Millville.

important component of the eustatic estimates of *Kominz et al.* [2008].

4. Integrated Stratigraphy

4.1. Sequence Pa0

[24] Sequence Pa0 is only identified in one borehole at Island Beach, New Jersey [*Liu et al.*, 1997]. This sequence is assigned middle neritic environment based on the presence of consist clayey, quartzose glauconite sand. Sequence Pa0 is characterized by ~40% planktonic foraminifera and middle neritic benthic foraminifera, including *Cibicidoides alleni*.

4.2. Sequence Pa1a

[25] At Bass River, sequence Pa1a is a thin sequence consisting of glauconitic clay and glauconitic sand (1258.7–1256.5 ft (383.7–383.0 m; Figure 5)). The sequence boundary at 1258.7 (383.7 m) is distinguished by clayey glauconitic sand overlain by glauconitic clay. The sequence boundary at 1256.5 ft (383.0 m) is similar to its older counterpart, with glauconitic clay overlying clayey glauconitic sand. No samples were taken from sequence Pa1 at Bass River due to its thinness and proximity to the K/P boundary. However, *Olsson et al.* [2002] assigned this interval a paleodepth of 100 m using a similar integrated stratigraphic approach as this work.

[26] At Ancora, sequence Pa1a consists of clayey glauconite sand from 612.5 to 606.5 ft (186.7–184.9 m; Figure 6). The sequence boundary at 612.5 ft (186.7 m) is marked by clayey glauconite sand overlain by slightly clayier glauconite sand. The quartz content slightly increases toward the sequence boundary at 606.5 ft (184.9 m). Biofacies A is more dominant than biofacies B at the base of the sequence. We estimate paleodepths rose to a peak of ~75 m associated with an increase in clay, followed by a 25 m shallowing due to a minor increase in the dominance of biofacies A, increase in quartz, decrease in glauconite and decreasing percent planktonic foraminifera from 65% to 55%.

[27] At Sea Girt, sequence Pa1a (497.5–482.4 ft (151.64–147.04 m)) is micaceous interbedded glauconitic silty clay and clayey silt with glauconite sand burrows (Figures 4 and 7). The lower sequence boundary (497.5 ft; 151.64 m) is identified by glauconitic silty clay overlying burrowed silty glauconite sand. The sequence becomes shallower upsection with a sandier, more glauconitic lithology near the sequence boundary at 482.4 ft (147.04 m).

[28] Sequence Pa1a (61.1–61.7 Ma) is assigned to planktonic foraminiferal Zone P1c and nannoplankton Zone NP4 [*Miller et al.*, 1998]. Sequence ages at each site are primarily based on nannoplankton and planktonic foraminiferal zonation and sedimentation estimates from site reports of *Miller et al.* [1998, 1999, 2006] and *Sugarman et al.* [2005] (auxiliary material).[1]

4.3. Sequence Pa1b

[29] At Millville, sequence Pa1b (981–974.9 ft (299.0–297.2 m)) is quartzose glauconite sand with weathered glauconite (Figure 8). The base of sequence at 981 ft (299.0 m) is inferred based on the presence of small clay rip-up clast in glauconitic sand. The upper boundary at 974.9 ft (297.2 m) is inferred based on the presence of clayey glauconitic sand overlying micaceous quartzose glauconitic sand. Biofacies C dominates up to the sequence boundary at 974.9 ft (297.2 m). At the upper boundary the dominance of biofacies A and a decrease in percent planktonic foraminifers indicate shallowing. We estimate paleodepths of ~90 m and a 20 m shallowing toward the top of sequence Pa1b.

[30] At Sea Girt, sequence Pa1b (482.4–469.8 ft (147.04–143.20 m)) is glauconite sand and silt at the base overlain by silty glauconitic fine quartz sand. The base of the sequence is identified by an indurated zone and pyrite nodule. Glauconite increases upsection to a lithologic change from slightly micaceous glauconitic sandy silt to silty glauconite-quartz sand at 480 ft (146.61 m). We estimate paleodepths were ~70 m for Pa1b.

[1] Auxiliary material data sets are available at ftp://ftp.agu.org/apend/pa/2009pa001800. Other auxiliary material files are in the HTML.

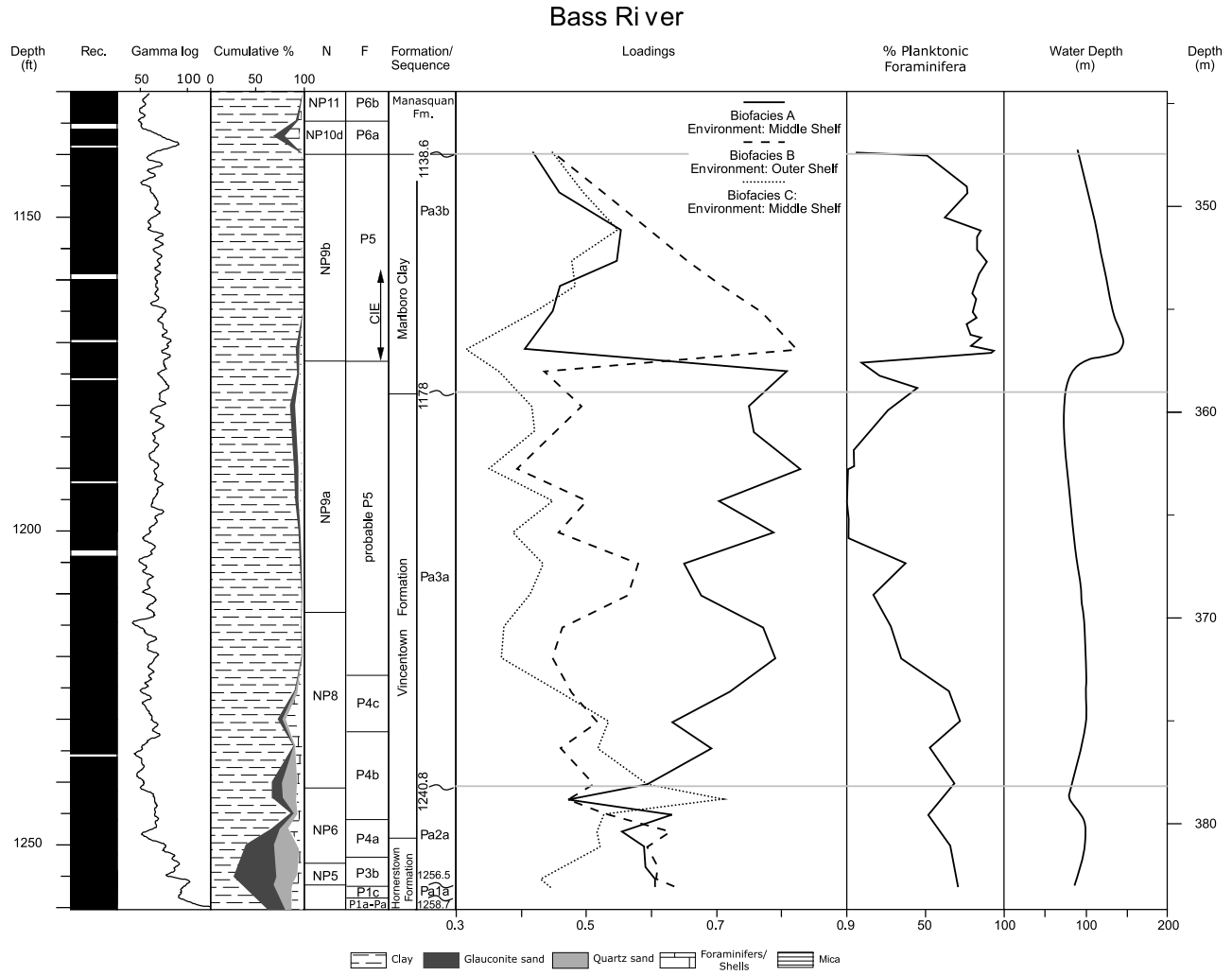

Figure 5. Recovery, gamma-ray, cumulative percent lithology, biostratigraphy and sequence boundary location of Paleocene strata at Bass River, NJ, with paleodepth curve derived from benthic foraminiferal biofacies paleoslope modeling, percent planktonic foraminifera, and lithology at Bass River, NJ. Horizontal gray lines across figure represent sequence boundary location. N, nannoplankton Zone and P, Planktonic foraminifera Zone.

[31] Sequence Pa1b (59.7–60 Ma) at Millville and Sea Girt is assigned to planktonic foraminiferal Zone P3b and calcareous nannoplankton Zone NP4 [*Miller et al.*, 1999, 2006] (auxiliary material).

4.4. Sequence Pa2a

[32] At Bass River, sequence Pa2a (1256.5–1240.8 ft (383.0–378.2 m)) is dominantly clayey glauconitic sand (Figure 5). We infer a sequence boundary at 1240.8 ft (378.2 m) based on the presence of light gray glauconitic silty clay overlain by darker more glauconitic gray clayey silt. Biofacies B dominates in sequence Pa2a from 1256.5 (382.98 m) to the maximum flooding surface (MFS) at 1246 ft (379.8 m). The dominance of biofacies A above 1246 ft (379.7 m) coincides with a decline in glauconite, mica and percent planktonic foraminifera (70% to 54%). Biofacies C dominates the remainder of sequence Pa2a from 1244 to 1240.8 ft (379.2–378.2 m). Percentages of glauconitic sand and mica increase toward the sequence boundary at 1240.8 ft (378.2 m). Maximum paleodepth of sequence Pa2a was 80 m and shallowed 20 m toward the top of the sequence.

[33] At Ancora, sequence Pa2a extends from 606.5 ft (184.9 m) to 599 ft (182.6 m). Its boundaries are not easily observed lithologically because this section is clayey glauconite sand, but biofacies allow recognition and subdivision of this sequence (Figure 6). Biofacies A and B co-dominate at the base of the sequence. The percentage of planktonic foraminifers decreases from 65% at 606.5 ft (184.86 m) to 36% at 600 ft (182.88 m). Biofacies C dominates the upper part of sequence Pa2a up to the sequence boundary at 599 ft (182.6 m). We estimate paleodepths of ~70 m for sequence Pa2a and a ~25 m shallowing toward the top of the sequence.

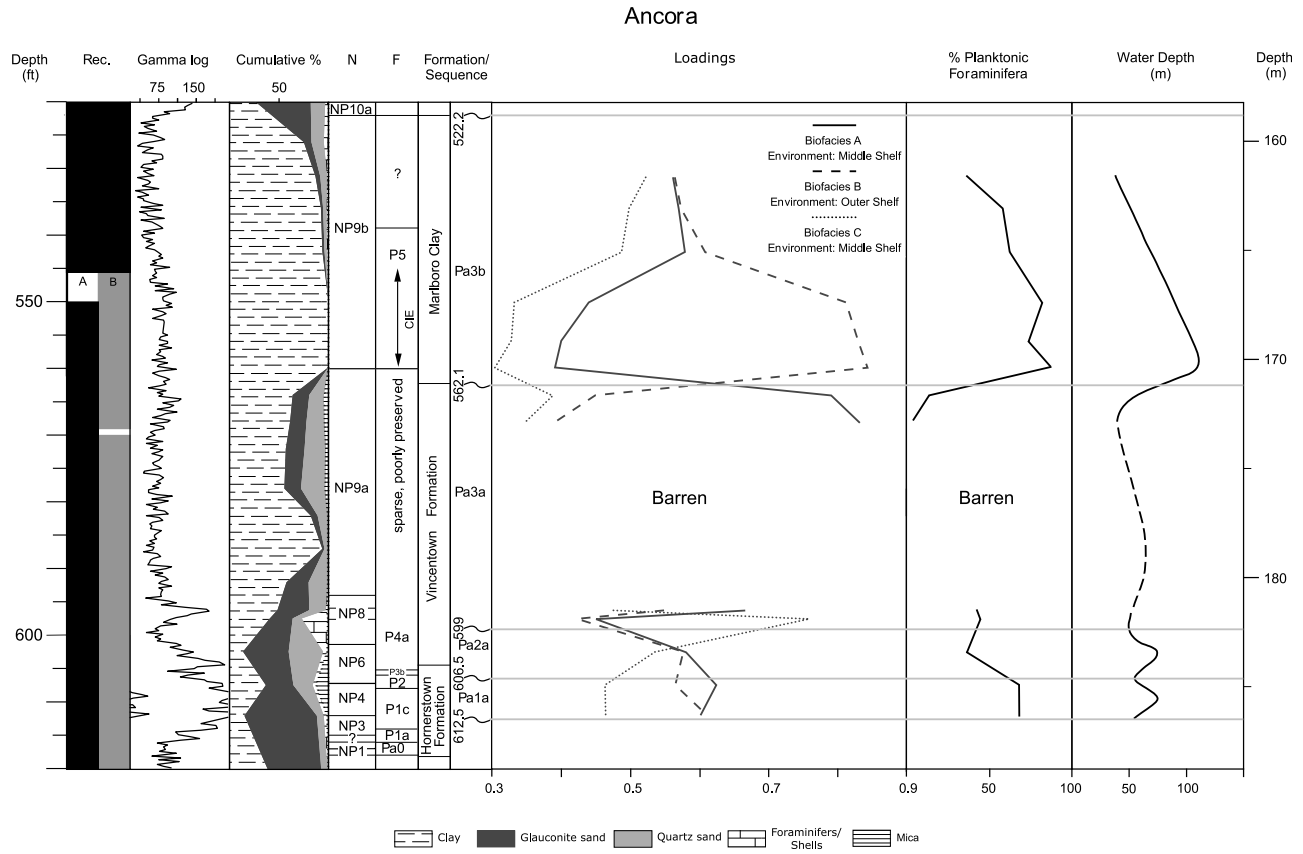

Figure 6. Recovery, gamma-ray, cumulative percent lithology, biostratigraphy, and sequence boundary location of Paleocene strata at Ancora, NJ, with paleodepth curve derived from benthic foraminiferal biofacies paleoslope modeling, percent planktonic foraminifera, and lithology at Ancora, NJ. Dashed portion of the paleodepth curve indicates values derived from lithology only due to dissolution of nannoplankton and foraminifers. Horizontal gray lines across figure represent sequence boundary location. N, nannoplankton Zone and P, Planktonic foraminifera Zone.

[34] At Sea Girt, sequence Pa2a (469.8–461.5 ft (143.20–140.67 m)) is glauconite sand with a layer of shell hash from 469.8 to 469 ft (143.20–142.95 m; Figures 4 and 7). The base of sequence Pa2a is characterized by quartzose glauconite sand overlain by glauconitic shell hash. Glauconite sand continues upsection with clay lined burrows from 466.2 to 463 ft (142.10 to 141.12 m). Paleodepths were ~65 m with a slight shallowing (10 m) toward to top of the sequence.

[35] Sequence Pa2a (58.6–57.9 Ma) at Bass River, Ancora, and Sea Girt belong to planktonic foraminiferal Zone P4a and nannoplankton Zone NP6 [*Miller et al.*, 1998, 1999, 2006; *Sugarman et al.*, 2005].

4.5. Sequence Pa2b

[36] At Millville, sequence Pa2b (974.9–959.4 ft (297.2–292.4 m)) is characterized by very clayey glauconite sand. Clay with pyrite and glauconitic sandy clayey silt underlay the sequence boundary at 974.9 ft (297.2 m; Figure 8). The dominance of biofacies C coincides with a decrease in percent planktonic foraminifers toward the sequence boundary at 959.4 ft (292.43 m). We estimate paleodepths were ~70 m and shallowed ~25 m toward to the top of the sequence.

[37] At Sea Girt, sequence Pa2b 461.5–445.6 ft (140.67–135.82 m) is slightly micaceous glauconitic sand and clay (Figures 4 and 7). The base of the sequence is marked by an irregular contact with glauconitic sandy clay overlain by glauconite sand. Glauconite and sand content decrease upsection to slightly micaceous glauconitic silty clay at 452 ft (137.77 m). Silty clays and clayey silts continue to the top of the sequence at 445.6 ft (135.82 m). Sequence Pa2b continues the shallowing trend of sequence Pa2a with paleodepths decreasing to ~50 m.

[38] Sequence Pa2b (57.1–57.5 Ma) at Millville and Sea Girt is assigned to planktonic foraminiferal Zone P4a and nannoplankton Zone NP7 [*Sugarman et al.*, 2005; *Miller et al.*, 2006] (auxiliary material).

4.6. Sequence Pa3a

[39] At Bass River, sequence Pa3a (1240.8–1178 ft (378.2–359.1 m)) consists of indurated silty, slightly glauconitic micaceous clay (Figure 5). Glauconite and mica content increase up section toward a sequence boundary identified at 1178 ft (359.1 m). Biofacies A dominates throughout sequence Pa3a. In this sequence, a notable rela-

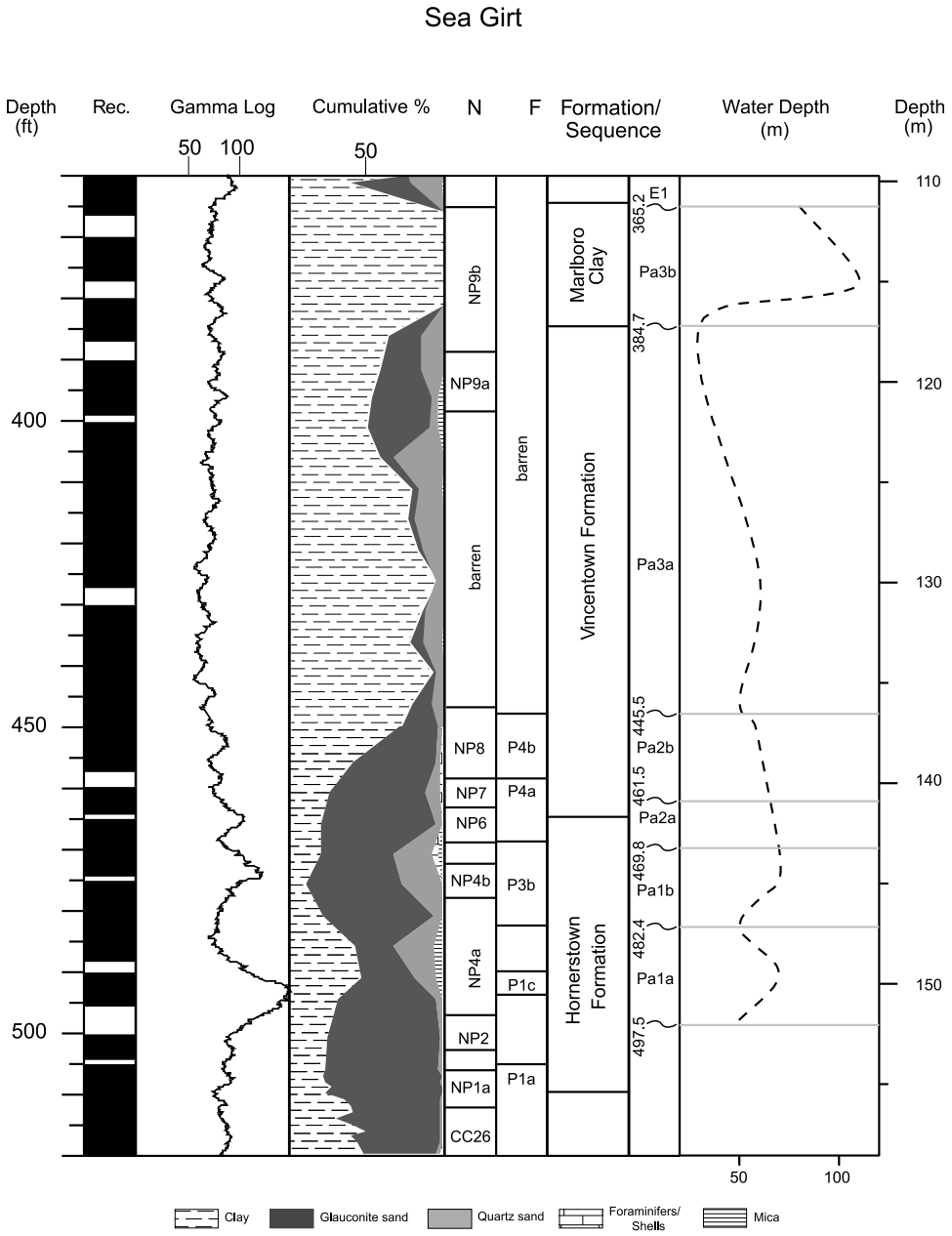

Figure 7. Recovery, gamma-ray, lithology, and biostratigraphy of Paleocene strata at Sea Girt, NJ, with paleodepth curve derived from lithology at Sea Girt, NJ. Dashed line indicates paleodepths were based on lithology due to an unsuitable amount of benthic foraminifers for assemblage analysis. N, nannoplankton Zone and P, Planktonic foraminifera Zone. Horizontal gray lines across figure represent sequence boundary location.

tionship occurs between biofacies A and percent planktonic foraminifera. A decrease in percent planktonic foraminifera from 72% at 1240.8 ft (378.2 m) to a few percent at 1200 ft (365.8 m) coincides with an increase in dominance of biofacies A upsection. The decrease in percent planktonic foraminifera may be due to dissolution. Yet, the decrease corresponds to a shallowing environment with slightly more sandy and glauconitic lithology. We estimate a paleodepths for sequence Pa3a were 100 m at the base and shallowing to 80 m on top.

[40] At Millville, sequence Pa3a (959.4–899.4 ft (292.4–274.1 m)) is micaceous, slightly glauconitic silty clay (Figure 8). The sequence boundary at 959.4 ft (292.43 m) is marked by irregular, heavily burrowed sandy clay with decreasing amounts of glauconite, mica, and quartz up to 950 ft (289.6 m). The silty clay increases with amounts of glauconite, mica and quartz from 950 ft (289.6 m) to 899.4 ft

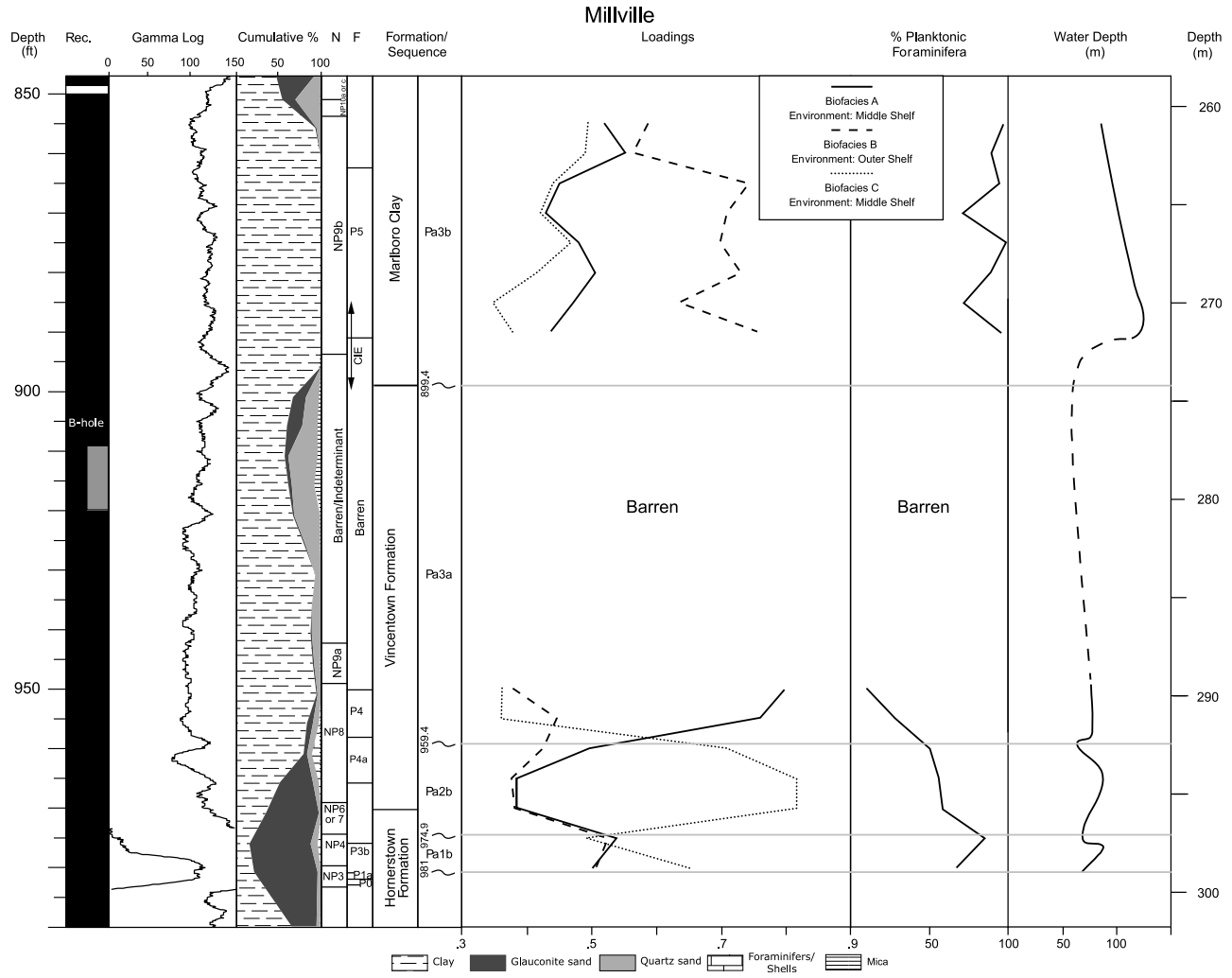

Figure 8. Recovery, gamma-ray, cumulative percent lithology, biostratigraphy, and sequence boundary location of Paleocene strata at Millville, NJ, with paleodepth curve derived from benthic foraminiferal biofacies paleoslope modeling, percent planktonic foraminifera, and lithology at Millville, NJ. Dashed portion of the paleodepth curve indicates values derived from lithology only due to dissolution of nannoplankton and foraminifers. Horizontal gray lines across figure represent sequence boundary location. N, nannoplankton Zone and P, Planktonic foraminifera Zone.

(273.83 m). At 899.4 ft (273.8 m) micaceous, glauconitic, sandy silt is overlain by clay interpreted as a sequence boundary. Biofacies A becomes dominant immediately above the sequence boundary at 959.4 ft (292.4 m). Much of sequence Pa3a is devoid of foraminifers at Millville due to dissolution, but the dominance of biofacies A compares well with results at Bass River and Ancora. The dominance of biofacies A correlates with a decrease in glauconite and a drop in percent planktonic foraminifera from 50% to 10% across the sequence boundary. We estimate paleodepths of ~60 m at the base and a shallowing to 40 m at the top of the sequence.

[41] At Ancora, sequence Pa3a (599–562.1 ft (182.6–171.3 m)) is clayey glauconite sand (Figure 6). An increase in clay content toward 595 ft (181.4 m) probably indicates the MFS. The lithology changes to glauconitic quartzose clay in the HST at 589 ft (179.5 m). At 580 ft (176.8 m) glauconite content increases and clay becomes slightly micaceous and silty. Biofacies A dominates all of sequence Pa3a. We estimate paleodepths were ~70 m for sequence Pa3a.

[42] At Sea Girt, sequence Pa3a (445.6–384.7 ft (135.82–117.26 m)) is slightly micaceous, slightly sandy, clayey silt or silty clay (Figures 4 and 7). At the base of the sequence the lithology is clayey silt to silty clay. Amounts of glauconite decrease upsection to 430 ft (131.1 m). The lithology coarsens upward from glauconitic silty clay at 430 ft (131.06 m) to slightly glauconitic micaceous clayey silt at 401 ft (122.22 m). The sandier lithology from 401 to 384.7 ft (122.22–117.26 m) represents the HST of sequence Pa3a. Paleodepths rose to ~60 m at 425 ft (130 m) and a shallowing to ~30 m occurred at the top of the sequence.

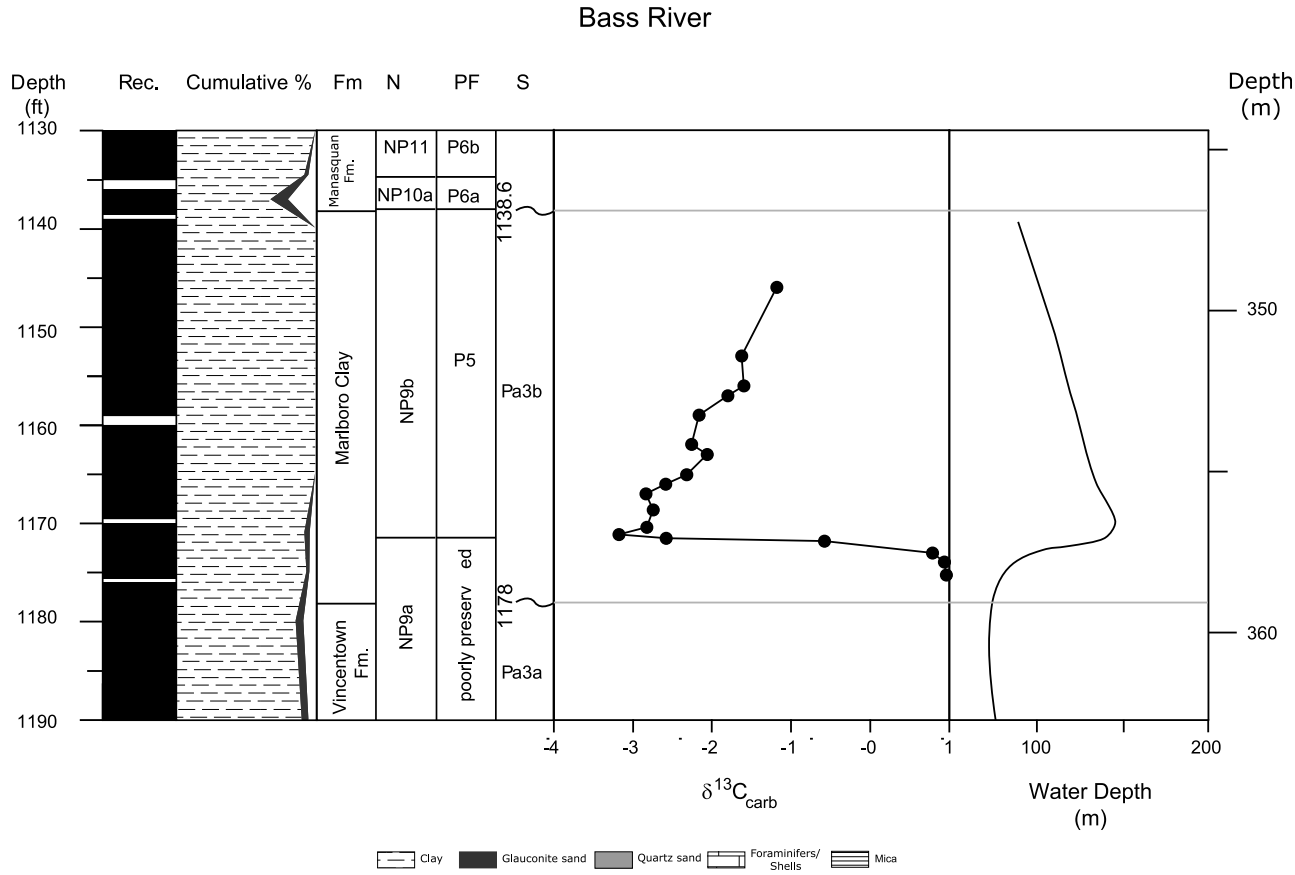

Figure 9. Recovery, lithology, and biostratigraphy of Paleocene strata at Bass River, NJ, with paleodepth curve and the location of the CIE. Carbon isotope measurements were on *Cibicidoides* spp. [*Cramer et al.*, 1999].

[43] Sequence Pa3a (55.8–56.6 Ma) at Bass River, Millville, Ancora, and Sea Girt is assigned to planktonic Zone P4c and nannoplankton NP9a [*Miller et al.*, 1998, 1999, 2006; *Sugarman et al.*, 2005] (auxiliary material).

4.7. Sequence Pa3b

[44] At Bass River, sequence Pa3b (1178–1138.6 ft (359.1–347.1 m)) is characterized by glauconitic micaceous silty clay overlain by massive dark greenish gray kaolinitic clay (Figure 5). The lithology remains clay up to the sequence boundary at 1138.6 ft (347.1 m) where the lithology changes to the very glauconitic clays of the Manasquan Formation. These greenish gray clays were deposited during the PETM and record the CIE (1173 ft; 357.5 m) near the base of the sequence [*Cramer et al.*, 1999; *Kent et al.*, 2003] (Figure 9). Biofacies A is dominant in glauconitic silty micaceous clay of the lower part of sequence Pa3b that. Biofacies B dramatically increases upsection, as it becomes the dominant factor at 1172.5 ft (357.4 m). The dominance of biofacies B accompanied with a dramatic increase in percent planktonic foraminifera (5% to 90%), massive green clays and decreasing amounts of glauconite sand documents a rapid large sea level rise from middle neritic environments (80 m) to outer neritic environments (~145 m) at 1172.5 ft (357.38 m). Percent planktonic foraminifers vary between 60% and 90% through most of sequence Pa3b and dramatically fall to 5% at the very top of the sequence.

[45] At Millville, sequence Pa3b contains brownish gray clay from 899.4 to 847 ft (273.8–258.2 m; Figure 8). At 899.4 ft (273.8 m) a sequence boundary occurs, with micaceous, glauconitic, sandy silt overlain by clay. The cumulative percent glauconite increases upsection toward the sequence boundary at 847 ft (258.2 m) where clays become slightly siltier. Sequence Pa3b is entirely dominated by biofacies B. This dominance is associated with relatively high percent planktonic foraminifera (70–97%). Paleodepth estimates for sequence Pa3b are 120 m.

[46] At Ancora (Figure 6), sequence Pa3b (562.1–522.2 ft (171.3–159.2 m)) contains greenish gray clay with convoluted bedding. The glauconitic, micaceous, clayey silt lithology makes the base of the sequence difficult to identify. However, we delineate the sequence boundary on the basis of an increase in foraminifers and decreasing amount mica and glauconite. The lithology shifts from clay to silty clay at 543.4 ft (165.6 m) with increasing amounts of glauconite, silt, and quartz toward the sequence boundary at 522.2 ft (171.3 m). The base of sequence Pa3b is dominated by inner neritic biofacies A (60 m paleodepth) up to 564.0 ft (171.9 m). The dominance of Biofacies B at 559.8 ft (170.6 m) denotes a paleodepth rise to ~110 m, which coincides with

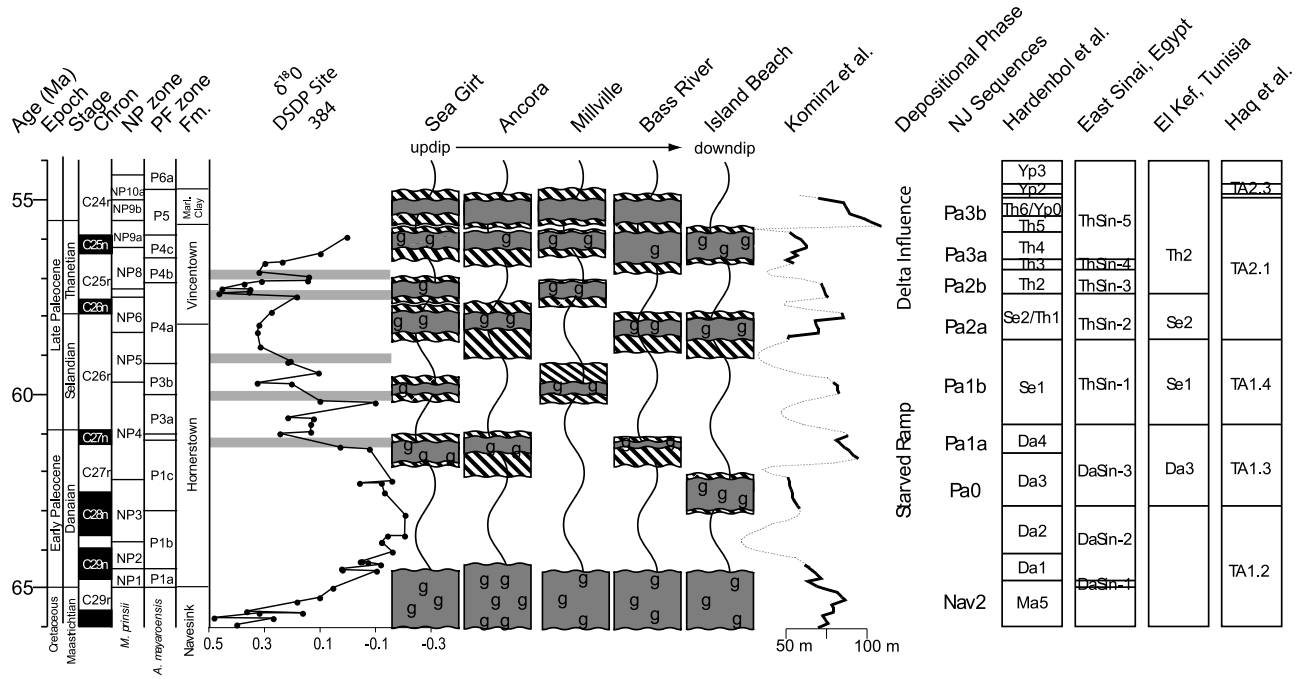

Figure 10. Distribution of Paleocene sediments on the New Jersey Coastal Plain calibrated to the *Berggren et al.* [1995] time scale with backstripped record of *Kominz et al.* [2008]. Paleocene hiatuses correlate to the benthic foraminifera δ^{18}O record of *Berggren et al.* [2000] at DSDP site 318, and sea level records of *Haq et al.* [1987], *Hardenbol et al.* [1998], *Luning et al.* [1998] (East Sinai), and *Guasti et al.* [2005] (El Kef, Tunisia). New Jersey core holes arranged based on paleoslope model projections. Gray rectangles with wavy lines represent sediments deposition, white areas show time not represented, and hatched areas are uncertainty in sequence boundary pick. Lower case "g" in sediments represents glauconite. Thick gray lines on the δ^{18}O record represent the increases in δ^{18}O that correlate to New Jersey hiatuses.

increasing clay lithology, percent planktonic foraminifera (90%).

[47] At Sea Girt (Figures 4 and 7), sequence Pa3b documents a sea level rise similar to those at Bass River, Ancora, and Millville, with burrowed glauconitic silty clay at 384.7 ft (117.26 m) rapidly changing to reddish brown clay at 380 ft (115.82 m). At 366.65 ft (111.8 m) the clay becomes greenish gray in color and continues to a burrowed contact zone at 365.9 ft (111.53 m). Paleodepths rose from ~30 m at the base of the sequence to ~100 m and shallowed ~20 m toward the top of the sequence.

[48] Sequence Pa3b (55.4–54.9 Ma) at Bass River, Millville, Ancora, and Sea Girt is belongs to planktonic foraminiferal Zone P5 and nannoplankton Zone NP9b [*Miller et al.*1998, 1999, 2006; *Sugarman et al.*, 2005] (auxiliary material).

5. Discussion

5.1. Global Correlation

[49] Foraminiferal biofacies and sequence stratigraphic studies of sediments at Bass River, Ancora, Millville, and Sea Girt, NJ allow us to delineate seven Paleocene–lowermost Eocene sequences in the New Jersey Coastal Plain. These seven sequences display paleodepth changes of ~20 m in less than a million years throughout the Paleocene. The formation of the Paleocene–lowermost Eocene sequence boundaries may result from tectonic lowering of base level and might not represent global lowering of sea level. However, simple subsidence and excellent regional coverage support the notion that thermoflexural subsidence dominates on the New Jersey Coastal Plain [*Kominz et al.*, 1998, 2008; *Miller et al.*, 2005a].

[50] We note the lateral discontinuity of New Jersey Paleocene sequences, but the cause is not well understood. Sequences are located in an updip location (continental shelf), mostly composed of glauconite, and are generally thin. This may lead to poor preservation of sequences, especially during base-level falls. However, comparisons to other localities suggest the New Jersey coastal plain has a robust Paleocene–lowermost Eocene record with sequence formation dominated by eustasy (Figure 10).

[51] To evaluate the role of eustasy as the major cause of water-depth changes during the Paleocene, we compare this study with other regional data sets [e.g., *Luning et al.*, 1998; *Guasti et al.*, 2005] and previously published eustatic estimates [e.g., *Haq et al.*, 1987; *Hardenbol et al.*, 1998]. In addition, we show a backstripped eustatic estimate derived from our water depth history backstripped by *Kominz et al.* [2008].

5.1.1. Correlation to Eustatic Records

[52] The New Jersey Coastal Plain displays seven sequences that favorably correlate to the global records of *Haq et al.* [1987] and *Hardenbol et al.* [1998] (Figure 10). Sequence Pa0 is only identified in one borehole in New Jersey (Island Beach). This sequence is assigned to Zones P1c and NP3, with the latter assignment discordant with sequence Pa1a assigned to Zones P1c and NP4 in three other core holes (Figure 10 and auxiliary material). We thus must allow for the possibility that this sequence is misdated at Island Beach. Nevertheless, sequence Pa0 corresponds well with sequence Da3 of *Hardenbol et al.* [1998] and sequence TA1.3 of *Haq et al.* [1987].

[53] Early Paleocene sequence Pa1a (Zones P1c and NP4) at Sea Girt, Ancora, and Bass River places within sequence TA1.3 of *Haq et al.* [1987] and correlates with Sequence Da4 of *Hardenbol et al.* [1998].

[54] Sequence Pa1b (Zones P3b and NP4) at Sea Girt and Millville correlates with sequence Sel1 of *Hardenbol et al.* [1998] and matches up well with Sequence TA1.4 of *Haq et al.* [1987].

[55] Sequence TA2.1 of *Haq et al.* [1987] is a long sequence that encompasses sequences Pa2a, Pa2b, Pa3a, and Pa3b (Figure 10). The *Hardenbol et al.* [1998] record displays six sequences in a similar time span that correlate well with the four upper Paleocene–lowermost Eocene sequences of New Jersey. Sequence Pa2a (Zones P4a and NP6) at Sea Girt, Ancora, Bass River, and Island Beach correlates well with sequence Sel2/Th1 of *Hardenbol et al.* [1998]. Sequence Pa2b (Zones P4a and NP7) at Sea Girt and Millville equates to Th2 of *Hardenbol et al.* [1998].

[56] Sequence Pa3a (Zones P4c and NP9a) was the only sequence identified in all of the New Jersey boreholes. The sequence at the downdip boreholes at Bass River and Island Beach are dated slightly older by ~0.4 Myr. However, Pa3a correlates well with sequence Th3 of *Hardenbol et al.* [1998].

[57] Sequence Pa3b is an early Eocene sequence (Zones NP9b and P5) whose base correlates with the onset of the CIE at Bass River and Ancora [e.g., *Cramer et al.*, 1999; *Kent et al.*, 2003]. It is marked by a major lithologic change from glauconite silts, sands and clays to massive kaolinitic clays. Sequence Pa3b displays excellent correlation with Th5 of *Hardenbol et al.* [1998].

5.1.2. Northern Africa

[58] *Luning et al.* [1998] identified seven Paleocene sequences in middle to outer shelf hemipelagic deposits in East Sinai, Egypt that display good correlation to the sequences of *Hardenbol et al.* [1998]. They utilized an integrated sequence stratigraphic methodology similar to ours to recognize the sequence stratigraphic framework and paleodepth history of Paleocene sediments. Sequences DaSin-3, ThSin-1, ThSin-2, ThSin-3, and ThSin-5 correlate quite well to the New Jersey record. However, the extents of the hiatuses in the East Sinai record have not been established (Figure 10). DaSin-3 correlates with sequences Pa0 and Pa1a. Sequence ThSin-1 also correlates well with sequence Pa1b of the New Jersey record. Sequences ThSin-2 and ThSin-3 have excellent correlation to sequences Pa2a and Pa2b, respectively. ThSin-4 was not resolved in NJ. Upper Paleocene sequence ThSin-5 compares well with sequences Pa3a.

[59] *Guasti et al.* [2005] identified four Paleocene sequence boundaries in El Kef, Tunisia that correlate well with sequences Th2, Sel2/Th1, Sel1 and Da3 of *Hardenbol et al.* [1998]. They performed an integrated analysis of dinocysts and benthic foraminiferal distribution patterns to characterize sea level and productivity fluctuations. Their paleodepths display a relative shallowing during the middle-late Paleocene similar to the New Jersey record, with outer neritic, open marine settings to more inner neritic settings. The sequence Da3 equivalent of *Guasti et al.* [2005] correlates with sequences Pa0 and Pa1a of New Jersey. Sequence Sel1 equivalent in Tunisia correlates to sequence Pa1b from New Jersey. The Sel2 equivalent correlates to sequence Pa2a. The Th2 equivalent correlates to sequences Pa2b of New Jersey.

5.2. Paleocene-Eocene Boundary

[60] The timing and magnitude of sea level changes associated with the PETM are of considerable interest because the extreme rapid warming (<10 kyr) of the whole ocean (5°C) may have been a major mechanism for eustatic rise. *Speijer and Morsi* [2002] estimated a ~20 m rise in sea level during the PETM based on ostracode assemblages in northern Africa. However, their estimates may reflect local paleodepths and they observed the need for additional localities to identify the eustatic change. An integrated sequence stratigraphic study by *Sluijs et al.* [2008] identified a rapid latest Paleocene to earliest Eocene rise in sea level at Bass River and Wilson Lake, NJ that they correlated to other sites in the North Sea, Central Arctic Ocean, and New Zealand, suggesting the rise was eustatic. *Sluijs et al.* [2008] demonstrated in the neritic sections they studied that PETM/CIE is within a sequence, with a rise in sea level leading the CIE. *Sluijs et al.* [2008] suggested the early rise in sea level may be due to establishment of the North Atlantic Igneous Provence (NAIP), with the melting of ice sheets in concert with steric effects contributing to maximum eustatic rise at the CIE. Based on these mechanisms of eustasy, *Sluijs et al.* [2008] estimated a 20–30 m eustatic rise based on these mechanisms across the P/E boundary.

[61] This study also supports the finding of *Sluijs et al.* [2008] that the PETM/CIE is bracketed by sequence boundaries (Figure 9). At Bass River, sequence Pa3b consists of inner neritic basal glauconite clay with 5% planktonic foraminifera just above the sequence boundary (1178 ft; 359.1 m) to outer neritic massive kaolinitic clay with 90% planktonic foraminifera at the CIE (1171 ft; 356.9 m), suggesting a large increase in paleodepths. At Bass River, the 7 ft (2.1 m) difference between the sequence boundary below and the CIE above is ~40 kyr using the average sedimentation rate for sequence Pa3b. This assumption of constant sediment rate in a sequence with major lithologic change is problematic (Figure 9).

[62] Amplitudes of the eustatic change during the CIE are uncertain. A backstripped estimates of our paleodepth changes is 60–80 m [e.g., *Kominz et al.*, 2008], which is significantly larger than the 20–30 m estimate of *Sluijs et al.* [2008]. We suggest that the integrated paleoslope model

presented here provides a valid estimate of paleodepth changes equivalent to quantitative analysis of nearshore dinocyst and terrestrially derived organic matter. Our ~60–70 m water depth rise is on par with 65 m paleodepths increase of *Olsson and Wise* [1987b] in New Jersey. Backstripped estimate of 60–80 m is also similar to that of *Haq et al.* [1987] for this interval, though it should be noted that their sea level estimates are typically ~2.5 times higher than New Jersey backstripped estimates. Nevertheless, it is clear that there is a major eustatic rise (at least 30 m) beginning before and continuing into the CIE. However, we must allow for the possibility that we have overestimated earliest Eocene paleodepths due to the unique depositional environment and paleoecological changes of the CIE (Figures 5–8). Our paleodepths are largely derived from benthic foraminifera, which experienced a 30–50% reduction in species at the CIE. Given that, we take the conservative estimate of the rise as 30 m [*Sluijs et al.*, 2008] to 60 m (this study).

[63] Mechanisms that would cause such a large eustatic rise are also debatable. *Sluijs et al.* [2008] attribute a 20–30 m eustatic rise across the P/E boundary to thermal expansion of the ocean, possible melting small Antarctic ice sheets and onset of the North Atlantic Igneous Provence.

[64] Injections of large igneous provinces (LIPS) associated with oceanic hot spots also affect sea level changes; *Pitman and Golovchenk*o [1983] estimated that the largest sea level change from LIPS would be ~50 m, but with relatively slow rates (<1 m/myr). Though the rates may actually be an order of magnitude higher (recognizing the rapid emplacement of LIPs), the calculations of such high amplitudes are for the largest of the LIPS (e.g., the Ontong Java Plateau which yielded $>50 \times 10^6$ km^3 of basalts, ca. 120 Ma [*Coffin and Eldholm*, 1994]). In contrast, the NAIP basalts that span the CIE were relatively modest in volume ($1–2 \times 10^6$ km^3 [*Roberts et al.*, 1984]) and would have had minimal effect on global sea level (~1–5 m).

[65] Thermal expansion of the ocean and ephemeral ice sheet fluctuations are the best candidates for eustatic change for the latest Paleocene to earliest Eocene. Whole ocean warming of 1°C would yield ~1 m sea level rise [e.g., *Miller et al.*, 2005b], this 5–6°C global warming [*Thomas and Shackleton*, 1996; *Zachos et al.*, 2003] would have caused 5–6 m of rise.

[66] Decay of ephemeral ice sheets stands as the most logical explanation for the rapid large eustatic rise during the latest Paleocene to earliest Eocene. Continental ice sheets produce high amplitude (200 m), rapid eustatic changes (20 m/kyr). *Miller et al.* [2005b] estimate 20–30 m eustatic changes during the Greenhouse were caused by ice volume changes.

[67] The estimated eustatic rise for the latest Paleocene–earliest Eocene is ~30–60 m [*Sluijs et al.*, 2008; *Kominz et al.*, 2008] (also this study). At the upper limits, ~10 m of the rise could be attributed to thermal expansion and emplacement of LIPs. This suggests the remaining 20–50 m rise is due to melting of small ice sheets. Therefore, the volumes of ice sheets during the latest Paleocene–earliest Eocene were ~30–75% ($8–21 \times 10^6$ km^3) modern values (27.6×10^6 km^3 [*Lythe et al.*, 2001]). This estimate is consistent with *Miller et al.*'s [2005b] estimate of ice volume during the "Greenhouse" world ($8–12 \times 10^6$ km^3). However, the upper end of our ice volume estimate may be too high.

[68] The paleobathymetric estimates presented here are consistent both laterally and vertically following Wathers law throughout all Paleocene sequences; generally ~20 m change. The large 60 m rise that spans the PETM is derived from the large benthic biofacies changes that we consider to be more reliable than previous estimates based on dinocyst, that largely reflect distance to shore and can be biased by nearshore processes [*Sluijs et al.*, 2008]. However, we cannot exclude the possibility that our benthic foraminiferal estimate of 60 m is biased by the dramatic nature of the PETM event; 1) there is a large turnover in benthic foraminifers at the time, though it was in primarily deep water (>200 m [*Tjalsma and Lohmann*, 1983; *Thomas*, 1990]); 2) there is a dramatic change in lithofacies to a kaolinitic clay [*Gibson et al.*, 1993; *Cramer et al.*, 1999; *Kopp et al.*, 2009]; and 3) there may have been an order of magnitude increase in sedimentation rates [*Cramer et al.*, 1999; *John et al.*, 2008; *Kopp et al.*, 2009; *Sluijs et al.*, 2008]. Nevertheless, the dramatic faunal, litho-, and sequence stratigraphic changes argue for a greater than "normal" (i.e., 15–25 m changes in sea level in other Paleocene sequences) rise in sea level.

5.3. Glacioeustasy During the Paleocene–Earliest Eocene

[69] Comparison of the New Jersey record with the eustatic and regional records of *Haq et al.* [1987], *Hardenbol et al.* [1998], *Luning et al.* [1998], and *Guasti et al.* [2005] suggests a eustatic mechanism for sequence development. The eustatic lowerings during the Paleocene are too fast and large to be explained by mechanisms other than ice-volume changes [*Miller et al.*, 2005b]. This is especially true when we consider that these sea level changes reconstructed from the New Jersey margin are minimal estimates due to clipping of LSTs [*Kominz et al.*, 2008] (Figure 10). *Miller et al.* [2005b] estimate 20–30 m eustatic changes during the Greenhouse were caused by ephemeral ice sheets ($8–12 \times 10^6$ km^3) restricted to high latitude locations on Antarctica. In the context of a hypothesized glacioeustatic origin of the Paleocene sequences, it is intriguing that the sequence boundaries occur at ~1.2 Myr intervals (i.e., 7 sequences in 8 Myr), consistent with a principal amplitude modulation of obliquity-sourced insolation variations.

[70] Paleocene glacioeustasy can be tested by correlating deep-sea oxygen isotope increases to sequence boundaries. Such studies have been done for the Cretaceous and Eocene-Miocene sections in New Jersey [*Pekar and Miller*, 1996; *Browning et al.*, 1996; *Miller et al.*, 2005a, 2005b; *Mizintseva et al.*, 2009]. Preliminary comparisons with the Paleocene benthic foraminiferal δ^{18}O record of *Berggren et al.* [2000] from DSDP Site 384 (W. North Atlantic; 3000 m paleodepths) are consistent with a glacioeustatic cause for the sea level changes. The magnitudes of eustatic falls are calculated from *Fairbanks and Matthews* [1978] δ^{18}O sea level calibration (0.11‰/10 m; Table 2). There is a level of uncertainty using this Pleistocene calibration because it may not apply to a greenhouse world when the mean δ^{18}O values

Table 2. The $\delta^{18}O$ Increases From *Berggren et al.* [2000] Record Correlated to New Jersey Sequences With Estimates of Sea Level Change Following the Methodology of *Pekar et al.* [2002]

Sequence	Age (Ma)	$\Delta^{18}O$	Δ Glacioeustasy (m)
Pa3a	56.2	0.18	10
Pa2b	57.5	0.28	15
Pa2a	58.4	0.22	12
Pa1b	60.0	0.43	22

are higher than present [*Miller et al.*, 2005b]. The Oligocene 0.1‰/10 m calibrations of *Pekar et al.* [2002] may be more appropriate for the Paleocene, though it only changes amplitudes by 2–4 m.

[71] Apportioning the $\delta^{18}O$ changes of glacioeustasy versus temperature is the main uncertainty in ice volume estimates. An independent proxy for temperature (e.g., Mg/Ca) is needed to delineate how much of the $\delta^{18}O$ record reflects ice volume changes. For the purposes of comparison we assume 50% of the $\delta^{18}O$ increases observed were due to temperature [*Pekar et al.*, 2002] (Figure 10).

[72] Oxygen isotope increases are correlated with the bases of sequences Pa1b, Pa2a, Pa2b, and Pa3a (60, 58.4, 57.5, 56.2 Ma, respectively; Table 2). Oxygen isotopic data are not sufficient for evaluating a link with the Pa0 and Pa1a sequence boundaries, although several points are suggestive of an increase. There is a major $\delta^{18}O$ increase (0.43‰, 22 m sea level fall) that correlates with the base of the Pa1b sequence boundary at Sea Girt and Millville, but the full extent of the increase continues through the placement of the sequence. This is possibly due to a minor correlation problem (~0.5 Myr). The $\delta^{18}O$ increases of 0.22‰ (12 m sea level fall) and 0.28‰ (15 m sea level fall) are correlative with the bases of sequences Pa2a and Pa2b, respectively. An oxygen isotope increase of 0.18‰ (10 m sea level fall) is correlative with the base of sequence Pa3a. Thus, we conclude there is good correlation between $\delta^{18}O$ increases in the deep sea and our sequence boundaries.

[73] One of the more interesting features of the $\delta^{18}O$ record is the 0.5‰ decrease from ~66 to 64 Ma associated with the Nav2 sequence. The Nav2 sequence spans the K/P boundary and highlights the paleoecologic and sea level changes associated with the boundary [see *Olsson et al.*, 2002]. This suggests a 2°C warming with 50 m sea level rise occurred over this time period. However, we observe a 20 m rise in sea level with a subsequent 30 m fall over the same interval. This observation is consistent with glacioeustasy and suggests a 1°C warming occurred.

[74] The early Paleocene rise in sea level predicted by oxygen isotopes suggests there should be sediment preservation on the New Jersey Coastal Plain. In fact, *Hardenbol et al.* [1998] record at least three early Paleocene sequences (Da1, Da2, and Da3) where we record one (Pa0). The starved ramp depositional phase of the early Paleocene coupled with the base level lowerings observed by *Hardenbol et al.* [1998] may have eroded thin sequences deposited at the time. It is possible that at least two $\delta^{18}O$ increases were undetected in the record. However, the base level lowering associated with sequence Da3 observed in each of the records presented correlates with a slight increase in $\delta^{18}O$.

6. Conclusions

[75] Recently cored Paleocene to lowermost Eocene sediments (Bass River, Ancora, Millville, and Sea Girt NJ; ODP Leg 150X) reveal seven sequences in the Marlboro, Vincentown and the underlying Hornerstown Formations. Sequence boundaries were identified based on inferred unconformities, and variations in benthic foraminiferal biofacies. Sequences were dated using integrated calcareous nannoplankton and planktonic foraminiferal biostratigraphy. The depositional paleoenvironment for each sequence was interpreted using sequence stratigraphic interpretation, percent planktonic foraminifera, and benthic foraminiferal biofacies analysis. Factor analysis identified three distinct benthic foraminiferal assemblages. Biofacies A was preserved in middle-outer shelf paleoenvironments (~50–100 m). Biofacies B occupied outer shelf paleoenvironments (~100–150 m). Lithologic and planktonic foraminiferal data indicate that the assemblage was located at slightly deeper paleodepths than biofacies A. Biofacies C is a relatively shallow biofacies assigned to middle neritic paleoenvironments (~50–80 m).

[76] The sequence analysis presented here provides a higher resolution record than previous New Jersey Coastal Plain studies of *Olsson and Wise* [1987a, 1987b], *Olsson* [1991], and *Liu et al.* [1997]. However, there are consistencies in paleodepth values among these studies. Sequences show repetitive patterns of relatively deeper water, middle-outer shelf lithology and biofacies of transgressive systems tracts shallowing to middle to inner shelf highstand systems tracts. The sequence stratigraphy and benthic foraminiferal biofacies suggest that paleodepths were 50–100 m during the early Paleocene with 25 m water depth changes. We observe a mid-late Paleocene shallowing (~20 m) consistent with other Paleocene records [*Luning et al.*, 1998; *Guasti et al.*, 2005]. The shallowing trend reverses prior to CIE with a return to a relatively higher sea level ~120–145 m.

[77] The timing of the sequences we identified in New Jersey display excellent correlation to eustatic and regional records of *Haq et al.* [1987], *Hardenbol et al.* [1998], *Luning et al.* [1998], and *Guasti et al.* [2005]. Thus, we suggest a eustatic mechanism as the cause of sequence development during the Paleocene. Comparisons to the benthic foraminiferal $\delta^{18}O$ record of *Berggren et al.* [2000] show excellent correlation of 0.2–0.4‰ $\delta^{18}O$ increases with sequence boundaries. We conclude the >20 m eustatic changes in less than 1 Myr observed in regional and eustatic records represent the growth and decay of ephemeral ice sheets during the Paleocene.

[78] **Acknowledgments.** This research was supported by National Science Foundation (NSF) grants EAR 0307112 and 070778 to K. G. Miller and by the New Jersey Geological Survey. Cores were obtained by the New Jersey Coastal Plain Drilling Project (Ocean Drilling Program Legs 150X and 174AX), supported by the NSF Continental Dynamics and Ocean Drilling Programs and the New Jersey Geological Survey. Samples were provided by Ocean Drilling Program. We thank Peter Stassen, Pete Sadler, Craig Fulthorpe, and Robert Speijer for constructive reviews. We also thank A. A. Kulpecz, S. Mizintseva, and M.-P. Aubry for discussions.

References

Aubry, M.-P., B. S. Cramer, K. G. Miller, J. D. Wright, D. V. Kent, and R. K. Olsson (2000), Late Paleocene event chronology: Unconformities, not diachrony, *Bull. Soc. Geol. Fr.*, *171*, 367–378, doi:10.2113/171.3.367.

Aubry, M.-P., et al. (2007), The Global Standard Stratotype-section and Point (GSSP) for the base of the Eocene series in the Dababiya section (Egypt), *Episodes*, *30*(4), 271–286.

Bains, S., R. M. Corfield, and R. D. Norris (1999), Mechanisms of climate warming at the end of the Paleocene, *Science*, *285*, 724–727, doi:10.1126/science.285.5428.724.

Bandy, O. L., and R. Arnal (1960), Concepts in foraminiferal paleoecology, *Am. Assoc. Pet. Geol. Bull.*, *44*, 1921–1932.

Berggren, W. A., and J. Aubert (1975), Paleocene benthonic foraminiferal biostratigraphy, paleobiogeography and paleoecology of Atlantic-Tethyan regions: Midway-type fauna, *Palaeogeogr. Palaeoclimatol. Palaeoecol.*, *18*, 73–192, doi:10.1016/0031-0182(75)90025-5.

Berggren, W. A., D. V. Kent, C. C. Swisher, and M. P. Aubry (1995), A revised Cenozoic geochronology and chronostratigraphy, in *Geochronology, Time Scales, and Global Stratigraphic Correlations*, edited by W. A. Berggren et al., *Spec. Publ. SEPM Soc. Sediment. Geol.*, *54*, 129–212.

Berggren, W. A., M.-P. Aubry, M. van Fossen, D. V. Kent, R. D. Norris, and F. Quillévéré (2000), Integrated Paleocene calcareous plankton magnetobiochronology and stable isotope stratigraphy: DSDP Site 384 (NW Atlantic Ocean), *Palaeogeogr. Palaeoclimatol. Palaeoecol.*, *159*, 1–51, doi:10.1016/S0031-0182(00)00031-6.

Brotzen, F. (1948), *The Swedish Paleocene and Its Foraminiferal Fauna*, *Arsb. Sver. Geol. Unders.*, *493*, 140 pp.

Browning, J. V., K. G. Miller, and D. K. Pak (1996), Global implications of lower to middle Eocene sequence boundaries on the New Jersey coastal plain: The icehouse cometh, *Geology*, *24*, 639–642, doi:10.1130/0091-7613(1996)024<0639:GIOLTM>2.3.CO;2.

Browning, J. V., K. G. Miller, and R. K. Olsson (1997), Lower to middle Eocene benthic foraminiferal biofacies, lithostratigraphic units, and their relationship to the New Jersey coastal plain sequences, *Proc. Ocean Drill. Program Sci. Results*, *150X*, 207–228.

Browning, J. V., K. G. Miller, P. J. Sugarman, M. A. Kominz, P. P. McLaughlin, A. A. Kulpecz, and M. D. Feigenson (2008), 100 Myr record of sequences, sedimentary facies and sea level change from Ocean Drilling Program onshore coreholes, US mid-Atlantic coastal plain, *Basin Res.*, *20*, 227–248, doi:10.1111/j.1365-2117.2008.00360.x.

Coffin, M. F., and O. Eldholm (1994), Large igneous provinces: Crustal structure, dimensions, and external consequences, *Rev. Geophys.*, *32*, 1–36, doi:10.1029/93RG02508.

Cramer, B. S., M.-P. Aubry, K. G. Miller, R. K. Olsson, J. D. Wright, and D. V. Kent (1999), An exceptional chronologic, isotopic, and clay mineralogic record of the latest Paleocene thermal maximum, Bass River, NJ, ODP 174AX, *Bull. Soc. Geol. Fr.*, *170*, 883–897.

Cushman, J. A. (1951), Paleocene foraminifera of the Gulf Coastal Region of the United States and adjacent areas, *U.S. Geol. Surv. Prof. Pap.*, *232*, 1–75.

DeConto, R. M., and D. Pollard (2003), A coupled climate–ice sheet modeling approach to the early Cenozoic history of the Antarctic ice sheet, *Palaeogeogr. Palaeoclimatol. Palaeoecol.*, *198*, 39–52, doi:10.1016/S0031-0182(03)00393-6.

Dickens, G. R., J. R. O'Neil, D. K. Rea, and R. M. Owen (1995), Dissociation of oceanic methane hydrate as a cause of the carbon isotope excursion at the end of the Paleocene, *Paleoceanography*, *10*, 965–972, doi:10.1029/95PA02087.

Eldholm, O., and E. Thomas (1993), Environmental impact of volcanic margin formation, *Earth Planet. Sci. Lett.*, *117*, 319–329, doi:10.1016/0012-821X(93)90087-P.

Fairbanks, R. G., and R. K. Matthews (1978), The marine oxygen isotope record in Pleistocene coral, Barbados, West Indies, *Quat. Res.*, *10*, 181–196, doi:10.1016/0033-5894(78)90100-X.

Farley, K. A., and S. F. Eltgroth (2003), An alternative age model for the Paleocene-Eocene thermal maximum using extraterrestrial ^{3}He, *Earth Planet. Sci. Lett.*, *208*, 135–148, doi:10.1016/S0012-821X(03)00017-7.

Gibson, T. G., L. M. Bybell, and J. P. Owens (1993), Latest Paleocene lithologic and biotic event in neritic deposits of southwestern New Jersey, *Paleoceanography*, *8*, 495–514, doi:10.1029/93PA01367.

Gingerich, P. D. (2003), Mammalian responses to climate change at the Paleocene-Eocene boundary: Polecat Bench record in the northern Bighorn Basin, Wyoming, *Spec. Pap. Geol. Soc. Am.*, *369*, 463–478.

Guasti, E., T. J. Kouwenhoven, H. Brinkhuis, and R. P. Speijer (2005), Paleocene sea-level and productivity changes at the southern Tethyan margin (El Kef, Tunisia), *Mar. Micropaleontol.*, *55*, 1–17, doi:10.1016/j.marmicro.2005.01.001.

Haq, B. U., J. A. N. Hardenbol, and P. R. Vail (1987), Chronology of fluctuating sea levels since the Triassic, *Science*, *235*, 1156–1167, doi:10.1126/science.235.4793.1156.

Hardenbol, J., J. Thierry, M. B. Farley, T. Jacquin, P.-C. de Graciansky, and P. R. Vail (1998), Mesozoic and Cenozoic sequence chronostratigraphic framework of European basins, in *Mesozoic and Cenozoic Sequence Stratigraphy of European Basins*, edited by P.-C. de Graciansky et al., *Spec. Publ. SEPM Soc. Sediment. Geol.*, *60*, 3–13.

John, C. M., S. M. Bohaty, J. C. Zachos, A. Sluijs, S. Gibbs, H. Brinkhuis, and T. J. Bralower (2008), North American continental margin records of the Paleocene-Eocene thermal maximum: Implications for global carbon and hydrological cycling, *Paleoceanography*, *23*, PA2217, doi:10.1029/2007PA001465.

Johnson, R. G. (1972), Conceptual models of benthic marine communities, in *Models in Paleobiology*, edited by T. J. M. Schopf, pp. 174–189, Freeman, Cooper, San Francisco, Calif.

Katz, M. E., and K. G. Miller (1991), Early Paleogene benthic foraminiferal assemblages and stable isotopes in the Southern Ocean, *Proc. Ocean Drill. Program Sci. Results*, *114*, 481–512.

Katz, M. E., B. S. Cramer, G. S. Mountain, S. Katz, and K. G. Miller (2001), Uncorking the bottle: What triggered the Paleocene/Eocene thermal maximum methane release?, *Paleoceanography*, *16*, 549–562, doi:10.1029/2000PA000615.

Kennett, J. P., and L. D. Stott (1991), Abrupt deep-sea warming, palaeoceanographic changes and benthic extinctions at the end of the Palaeocene, *Nature*, *353*, 225–229, doi:10.1038/353225a0.

Kent, D. V., B. S. Cramer, L. Lanci, D. Wang, J. D. Wright, and R. Van der Voo (2003), A case for a comet impact trigger for the Paleocene/Eocene thermal maximum and carbon isotope excursion, *Earth Planet. Sci. Lett.*, *211*, 13–26, doi:10.1016/S0012-821X(03)00188-2.

Kominz, M. A., K. G. Miller, and J. V. Browning (1998), Long-term and short-term global Cenozoic sea-level estimates, *Geology*, *26*, 311–314, doi:10.1130/0091-7613(1998)026<0311:LTASTG>2.3.CO;2.

Kominz, M. A., J. V. Browning, K. G. Miller, P. J. Sugarman, S. Mizintseva, and C. R. Scotese (2008), Late Cretaceous to Miocene sea-level estimates from the New Jersey and Delaware coastal plain coreholes: An error analysis, *Basin Res.*, *20*, 211–226, doi:10.1111/j.1365-2117.2008.00354.x.

Kopp, R. E., D. Schumann, T. D. Raub, D. S. Powars, L. V. Godfrey, N. L. Swanson-Hysell, A. C. Maloof, and H. Vali (2009), An Appalachian Amazon? Magnetofossil evidence for the development of a tropical river-like system in the mid-Atlantic United States during the Paleocene-Eocene thermal maximum, *Paleoceanography*, *24*, PA4211, doi:10.1029/2009PA001783.

Kurtz, A. C., L. R. Kump, M. A. Arthur, J. C. Zachos, and A. Paytan (2003), Early Cenozoic decoupling of the global carbon and sulfur cycles, *Paleoceanography*, *18*(4), 1090, doi:10.1029/2003PA000908.

Liu, C., J. V. Browning, K. G. Miller, and R. K. Olsson (1997), Paleocene benthic foraminiferal biofacies and sequence stratigraphy, Island Beach borehole, New Jersey, *Proc. Ocean Drill. Program Sci. Results*, *150X*, 267–275.

Luning, S., A. M. Marzouk, and J. Kuss (1998), The Paleocene of central East Sinai, Egypt: "Sequence stratigraphy" in monotonous hemipelagites, *J. Foraminiferal Res.*, *28*, 19–39.

Lythe, M. B., D. G. Vaughn, and the BEDMAP Consortium (2001), BEDMAP: A new ice thickness and subglacial topographic model of Antarctica, *J. Geophys. Res.*, *106*, 11,335–11,351, doi:10.1029/2000JB900449.

Miller, K. G., R. G. Fairbanks, and G. S. Mountain (1987), Tertiary oxygen isotope synthesis, sea level history, and continental margin erosion, *Paleoceanography*, *21*, 1–19, doi:10.1029/PA002i001p00001.

Miller, K. G., et al. (1998), Bass River Site, *Proc. Ocean Drill. Program Initial Rep.*, *174AX*, 5–43.

Miller, K. G., et al. (1999), Ancora Site, *Proc. Ocean Drill. Program Initial Rep.*, *174AX*, suppl., 1–65.

Miller, K. G., P. J. Sugarman, J. V. Browning, M. A. Kominz, J. C. Hernández, R. K. Olsson, J. D. Wright, M. D. Feigenson, and W. Van Sickel (2003), Late Cretaceous chronology of large, rapid sea-level changes: Glacioeustasy during the greenhouse world, *Geology*, *31*, 585–588, doi:10.1130/0091-7613(2003)031<0585:LCCOLR>2.0.CO;2.

Miller, K. G., P. J. Sugarman, J. V. Browning, M. A. Kominz, R. K. Olsson, M. D. Feigenson, and J. C. Hernández (2004), Upper Cretaceous sequences and sea-level history, New Jersey

Coastal Plain, *Geol. Soc. Am. Bull.*, *116*, 368–393, doi:10.1130/B25279.1.

Miller, K. G., M. A. Kominz, J. V. Browning, J. D. Wright, G. S. Mountain, M. E. Katz, P. J. Sugarman, B. S. Cramer, N. Christie-Blick, and S. F. Pekar (2005a), The Phanerozoic record of global sea-level change, *Science*, *310*, 1293–1298, doi:10.1126/science.1116412.

Miller, K. G., J. D. Wright, and J. V. Browning (2005b), Visions of ice sheets in a greenhouse world, *Mar. Geol.*, *217*, 215–231, doi:10.1016/j.margeo.2005.02.007.

Miller, K. G., et al. (2006), Sea Girt Site, *Proc. Ocean Drill. Program Initial Rep.*, *174AX*, suppl., 1–104.

Mizintseva, S., J. V. Browning, and K. G. Miller (2009), Integrated late Santonian–early Campanian sequence stratigraphy, New Jersey coastal plain: Implications to global sea-level studies, *Stratigraphy*, *6*, 45–60.

Olsson, R. K. (1991), Cretaceous to Eocene sea-level fluctuations on the New Jersey margin, *Sediment. Geol.*, *70*, 195–208, doi:10.1016/0037-0738(91)90141-Y.

Olsson, R. K., and E. E. Nyong (1984), A paleoslope model for Campanian–lower Maestrichtian foraminifera of New Jersey and Delaware, *J. Foraminiferal Res.*, *14*, 50–68, doi:10.2113/gsjfr.14.1.50.

Olsson, R. K., and S. W. Wise Jr. (1987a), Upper Maestrichtian to middle Eocene stratigraphy of the New Jersey slope and coastal plain, *Initial Rep. Deep Sea Drill. Proj.*, *93*, 1343–1365.

Olsson, R. K., and S. W. Wise Jr. (1987b), Upper Paleocene to middle Eocene depositional sequences and hiatuses in the New Jersey Atlantic margin, in *Timing and Depositional History of Eustatic Sequences: Constraints on Seismic Stratigraphy*, edited by C. Ross and D. Haman, *Spec. Publ. Cushman Found. Foraminiferal Res.*, *24*, 99–112.

Olsson, R. K., K. G. Miller, J. V. Browning, J. D. Wright, and B. S. Cramer (2002), Sequence stratigraphy and sea-level change across the Cretaceous-Tertiary boundary on the New Jersey passive margin, *Spec. Pap. Geol. Soc. Am.*, *356*, 97–108.

Pak, D. K., and K. G. Miller (1992), Paleocene to Eocene benthic foraminiferal isotopes and assemblages: Implications for deepwater circulation, *Paleoceanography*, *7*, 405–422, doi:10.1029/92PA01234.

Pekar, S., and K. G. Miller (1996), New Jersey Oligocene "Icehouse" sequences (ODP Leg 150X) correlated with global $\delta^{18}O$ and Exxon eustatic records, *Geology*, *24*, 567–570, doi:10.1130/0091-7613(1996)024<0567:NJOISO>2.3.CO;2.

Pekar, S. F., N. Christie-Blick, M. A. Kominz, and K. G. Miller (2002), Calibration between eustatic estimates from backstripping and oxygen isotopic records for the Oligocene, *Geology*, *30*, 903–906, doi:10.1130/0091-7613(2002)030<0903:CBEEFB>2.0.CO;2.

Pitman, W. C., III, and X. Golovchenko (1983), The effect of sea-level change on the shelf edge and slope of passive margins, *Spec. Publ. Soc. Econ. Paleontol. Mineral.*, *33*, 41–58.

Plummer, H. J. (1926), *Foraminifera of the Midway Formation in Texas*, *Univ. Tex. Bull.*, *2644*, 206 pp.

Poag, C. W. (1980), Foraminiferal stratigraphy, paleoenvironments, and depositional cycles in the outer Baltimore Canyon Trough, in *Geological Studies of the COST No. B-3 Well: United States Mid-Atlantic Continental Slope Area*, edited by P. A. Scholle, *U.S. Geol. Surv. Circ.*, *833*, 44–65.

Poag, C. W., and W. D. Sevon (1989), A record of Appalachian denudation in postrift Mesozoic and Cenozoic sedimentary deposits of the U.S. middle Atlantic continental margin, *Geomorphology*, *2*, 119–157, doi:10.1016/0169-555X(89)90009-3.

Roberts, D. G., J. Backman, A. C. Morton, J. W. Murray, and J. B. Keene (1984), Evolution of volcanic rifted margins: Synthesis of Leg 81 results on the west margin of Rockall Plateau, *Initial Rep. Deep Sea Drill. Proj.*, *81*, 883–911.

Röhl, U., T. J. Bralower, R. D. Norris, and G. Wefer (2000), New chronology for the late Paleocene thermal maximum and its environmental implications, *Geology*, *28*, 927–930, doi:10.1130/0091-7613(2000)28<927:NCFTLP>2.0.CO;2.

Royer, D. L., R. A. Berner, I. P. Montanez, N. J. Tabor, and D. J. Beerling (2004), CO_2 as a primary driver of Phanerozoic climate, *GSA Today*, *14*, 4–10, doi:10.1130/1052-5173(2004)014<4:CAAPDO>2.0.CO;2.

Savin, S. M. (1977), The history of the Earth's surface temperature during the past 100 million years, *Annu. Rev. Earth Planet. Sci.*, *5*, 319–355, doi:10.1146/annurev.ea.05.050177.001535.

Savin, S. M., R. G. Douglas, and F. G. Stehli (1975), Tertiary marine paleotemperatures, *Geol. Soc. Am. Bull.*, *86*, 1499–1510, doi:10.1130/0016-7606(1975)86<1499:TMP>2.0.CO;2.

Shackleton, N., and A. Boersma (1981), The climate of the Eocene ocean, *J. Geol. Soc. London*, *138*, 153–157, doi:10.1144/gsjgs.138.2.0153.

Sluijs, A., et al. (2008), Eustatic variations during the Paleocene-Eocene greenhouse world, *Paleoceanography*, *23*, PA4216, doi:10.1029/2008PA001615.

Speijer, R. P., and A.-M. M. Morsi (2002), Ostracode turnover and sea-level changes associated with the Paleocene-Eocene thermal maximum, *Geology*, *30*, 23–26, doi:10.1130/0091-7613(2002)030<0023:OTASLC>2.0.CO;2.

Steckler, M. S., and A. B. Watts (1978), Subsidence of the Atlantic-type continental margin off New York, *Earth Planet. Sci. Lett.*, *41*, 1–13, doi:10.1016/0012-821X(78)90036-5.

Steckler, M. S., G. S. Mountain, K. G. Miller, and N. Christie-Blick (1999), Reconstruction of Tertiary progradation and clinoform development on the New Jersey passive margin by 2-D backstripping, *Mar. Geol.*, *154*, 399–420, doi:10.1016/S0025-3227(98)00126-1.

Storey, M., R. A. Duncan, and C. C. Swisher III (2007), Paleocene-Eocene thermal maximum and the opening of the northeast Atlantic, *Science*, *316*, 587–589, doi:10.1126/science.1135274.

Sugarman, P. J., et al. (2005), Millville Site, *Proc. Ocean Drill. Program Initial Rep.*, *174AX*, suppl., 1–94.

Svensen, H., S. Planke, A. Malthe-Sørensen, B. Jamtveit, R. Myklebust, T. R. Eidem, and S. S. Rey (2004), Release of methane from a volcanic basin as a mechanism for initial Eocene global warming, *Nature*, *429*, 542–545, doi:10.1038/nature02566.

Thomas, D. J., J. C. Zachos, T. J. Bralower, E. Thomas, and S. Bohaty (2002), Warming the fuel for the fire: Evidence for the thermal dissociation of methane hydrate during the Paleocene-Eocene thermal maximum, *Geology*, *30*, 1067–1070, doi:10.1130/0091-7613(2002)030<1067:WTFFTF>2.0.CO;2.

Thomas, E. (1990), Late Cretaceous–early Eocene mass extinctions in the deep sea, *Spec. Pap. Geol. Soc. Am.*, *247*, 481–495.

Thomas, E., and N. J. Shackleton (1996), The Palaeocene-Eocene benthic foraminiferal extinction and stable isotope anomalies, in *Correlation of the Early Paleogene in Northwestern Europe*, edited by R. W. O. Knox, R. M. Corfield, and R. E. Dunam, *Geol. Soc. Spec. Publ.*, *101*, 401–441.

Tjalsma, R. C., and G. P. Lohmann (1983), *Paleocene-Eocene Bathyal and Abyssal Benthic Foraminifera From the Atlantic Ocean*, *Micropaleontol. Spec. Publ.*, *4*, 1–90.

Van der Zwaan, G. J., I. A. P. Duijnstee, M. den Dulk, S. R. Ernst, N. T. Jannik, and T. J. Kouwenhoven (1999), Benthic foraminifers: Proxies or problems? A review of paleocological concepts, *Earth Sci. Rev.*, *46*, 213–236, doi:10.1016/S0012-8252(99)00011-2.

van Morkhoven, F. P. C. M., W. A. Berggren, and A. S. Edwards (1986), Cenozoic cosmopolitan deep-water benthic foraminifera, *Bull. Cent. Rech. Explor. Prod. Elf Aquitaine*, *11*, 329–426.

Zachos, J., M. Pagani, L. Sloan, E. Thomas, and K. Billups (2001), Trends, rhythms, and aberrations in global climate 65 Ma to present, *Science*, *292*, 686–693, doi:10.1126/science.1059412.

Zachos, J. C., M. W. Wara, S. M. Bohaty, M. L. Delaney, M. Rose-Petrizzo, A. Brill, T. J. Bralower, and I. Premoli-Silva (2003), A transient rise in tropical sea surface temperature during the Paleocene-Eocene thermal maximum, *Science*, *302*, 1551–1554, doi:10.1126/science.1090110.

Zachos, J. C., S. Schouten, S. Bohaty, T. Quattlebaum, A. Sluijs, H. Brinkhuis, S. J. Gibbs, and T. J. Bralower (2006), Extreme warming of mid-latitude coastal ocean during the Paleocene-Eocene thermal maximum: Inferences from TEX_{86} and isotope data, *Geology*, *34*, 737–740, doi:10.1130/G22522.1.

J. V. Browning, K. G. Miller, R. K. Olsson, and J. D. Wright, Department of Earth and Planetary Sciences, Rutgers, State University of New Jersey, Piscataway, NJ 08854, USA.

B. S. Cramer, Department of Geological Sciences, University of Oregon, Eugene, OR 97403, USA.

A. D. Harris, Chevron Corporation, 1500 Louisiana St., Houston, TX 77002, USA. (harris.ad@gmail.com)

P. J. Sugarman, New Jersey Geological Survey, Trenton, NJ 08625, USA.